UNIVERSIDAD DE INVESTIGACIÓN DE TECNOLOGÍA EXPERIMENTAL YACHAY

Escuela de Ciencias Químicas e Ingeniería

Synthesis and characterization of hydrogels formed by PVA-VAVTD-KOH used in Zn batteries

Trabajo de integración curricular presentado como requisito para la obtención del título de Ingeniero en Polímeros

Autor:

Reyes Jacome Edwin Steven

Tutores:

Ph.D. Tafur Guisao Juan Pablo

Ph.D. Fernández Romero Antonio J.

Urcuquí, Junio 2021

SECRETARÍA GENERAL
(Vicerrectorado Académico/Cancillería)
ESCUELA DE CIENCIAS QUÍMICAS E INGENIERÍA
CARRERA DE POLÍMEROS
ACTA DE DEFENSA No. UITEY-CHE-2021-00013-AD

A los 24 días del mes de junio de 2021, a las 10:00 horas, de manera virtual mediante videoconferencia, y ante el Tribunal Calificador, integrado por los docentes:

Presidente Tribunal de Defensa	Dr. DIAZ BARRIOS, ANTONIO , Ph.D.
Miembro No Tutor	Dra. MICHELL URIBE, ROSE MARY RITA , Ph.D.
Tutor	Dr. TAFUR GUISAO, JUAN PABLO , Ph.D.

El(la) señor(ita) estudiante **REYES JACOME, EDWIN STEVEN**, con cédula de identidad No. **1719639724**, de la **ESCUELA DE CIENCIAS QUÍMICAS E INGENIERÍA**, de la Carrera de **POLÍMEROS**, aprobada por el Consejo de Educación Superior (CES), mediante Resolución **RPC-SO-41-No.476-2014**, realiza a través de videoconferencia, la sustentación de su trabajo de titulación denominado: **Synthesis and characterization of hydrogels formed by PVA-VAVTD-KOH used in Zn batteries**, previa a la obtención del título de **INGENIERO/A DE POLÍMEROS**.

El citado trabajo de titulación, fue debidamente aprobado por el(los) docente(s):

Tutor	Dr. TAFUR GUISAO, JUAN PABLO , Ph.D.

Y recibió las observaciones de los otros miembros del Tribunal Calificador, las mismas que han sido incorporadas por el(la) estudiante.

Previamente cumplidos los requisitos legales y reglamentarios, el trabajo de titulación fue sustentado por el(la) estudiante y examinado por los miembros del Tribunal Calificador. Escuchada la sustentación del trabajo de titulación a través de videoconferencia, que integró la exposición de el(la) estudiante sobre el contenido de la misma y las preguntas formuladas por los miembros del Tribunal, se califica la sustentación del trabajo de titulación con las siguientes calificaciones:

Tipo	Docente	Calificación
Tutor	Dr. TAFUR GUISAO, JUAN PABLO , Ph.D.	10,0
Presidente Tribunal De Defensa	Dr. DIAZ BARRIOS, ANTONIO , Ph.D.	10,0
Miembro Tribunal De Defensa	Dra. MICHELL URIBE, ROSE MARY RITA , Ph.D.	9,8

Lo que da un promedio de: **9.9 (Nueve punto Nueve)**, sobre 10 (diez), equivalente a: **APROBADO**

Para constancia de lo actuado, firman los miembros del Tribunal Calificador, el/la estudiante y el/la secretario ad-hoc.

Certifico que *en cumplimiento del Decreto Ejecutivo 1017 de 16 de marzo de 2020, la defensa de trabajo de titulación (o examen de grado modalidad teórico práctica) se realizó vía virtual, por lo que las firmas de los miembros del Tribunal de Defensa de Grado, constan en forma digital*.

REYES JACOME, EDWIN STEVEN
Estudiante

Dr. DIAZ BARRIOS, ANTONIO , Ph.D.
Presidente Tribunal de Defensa

ANTONIO DIAZ BARRIOS
Firmado digitalmente por ANTONIO DIAZ BARRIOS
Fecha: 2021.06.24 14:14:55

JUAN PABLO TAFUR GUISAO
Firmado digitalmente por JUAN PABLO TAFUR GUISAO
Fecha: 2021.06.24 13:35:47 -05'00'

Dr. TAFUR GUISAO, JUAN PABLO , Ph.D.
Tutor

Dra. MICHELL URIBE, ROSE MARY RITA , Ph.D.
Miembro No Tutor

YASELGA NARANJO, CARLA
Secretario Ad-hoc

Dra. MICHELL URIBE, ROSE MARY RITA , Ph.D.

AUTORÍA

Yo, EDWIN STEVEN REYES JACOME, con cédula de identidad 1719639724, declaro que las ideas, juicios, valoraciones, interpretaciones, consultas bibliográficas, definiciones y conceptualizaciones expuestas en el presente trabajo; así cómo, los procedimientos y herramientas utilizadas en la investigación, son de absoluta responsabilidad de el/la autora (a) del trabajo de integración curricular. Así mismo, me acojo a los reglamentos internos de la Universidad de Investigación de Tecnología Experimental Yachay.

Urcuquí, junio de 2021

_____

Edwin Steven Reyes Jacome

CI: 1719639724

AUTORIZACIÓN DE PUBLICACIÓN

Yo, EDWIN STEVEN REYES JACOME, con cédula de identidad 1719639724, cedo a la Universidad de Tecnología Experimental Yachay, los derechos de publicación de la presente obra, sin que deba haber un reconocimiento económico por este concepto. Declaro además que el texto del presente trabajo de titulación no podrá ser cedido a ninguna empresa editorial para su publicación u otros fines, sin contar previamente con la autorización escrita de la Universidad.

Asimismo, autorizo a la Universidad que realice la digitalización y publicación de este trabajo de integración curricular en el repositorio virtual, de conformidad a lo dispuesto en el Art. 144 de la Ley Orgánica de Educación Superior

Urcuquí, junio de 2021

Edwin Steven Reyes Jacome

CI: 1719639724

DEDICATORIA

A mi familia por formarme como el hombre que soy y

nunca dejarme caer sin importar que tan duro sea el camino.

Son el regalo más grande que me ha dado la vida.

Gracias por todo.

Edwin Steven Reyes Jacome

AGRADECIMIENTOS

Como todo en la vida lo primero que deseo hacer es dar las gracias a toda mi familia ya que, sin su apoyo, confianza y entrega no pudiese haber llegado donde estoy ahora. Aquellos sacrificios grandes y pequeños que hicieron por mí están guardados en el fondo de mí corazón y los recompensaré con toda mi fuerza. De igual forma deseo agradecer a mis tutores de tesis, el PhD. Juan Pablo Tafur y el PhD. Antonio J. Fernández Romero por brindarme su guía y tutela para crecer en el mundo académico. Poco a poco espero seguir dando pasos firmes para introducirme en el mundo de la investigación gracias a ustedes. Al Dr. Antonio Díaz Barrios deseo darle mi más profundo agradecimiento por todos los años de enseñanza y por introducirme al maravilloso mundo de los polímeros.

Finalmente, pero no menos importante a mis amigos que han transformado aquellos malos momentos de la vida universitaria en una tarde de risas.

Edwin Steven Reyes Jacome

RESUMEN

Se realizó la síntesis de un gel polimérico formado por una mezcla de Poli (Vinil Alcohol) (PVA) y diferentes proporciones del ter-polímero compuesto de acetato de vinilo, acrilato de butilo y neodecanoato de vinilo (VAVTD). Los geles se doparon con Hidróxido de Potasio (KOH) mediante la inmersión del polímero en una disolución de KOH 12M por 24 horas, para su posterior caracterización por diferentes técnicas espectroscópicas, térmicas y electroquímicas. Las pruebas de difracción de rayos X demostraron una reducción en la cristalinidad del polímero tras ser sumergido en KOH. De igual forma, la prueba de voltametría cíclica demostró que a mayor proporción de VAVTD las intensidades de corriente alcanzadas aumentan llegando a un máximo de 310 mA con una membrana VAVTD/PVA (4:1). Los valores de intensidad obtenidos son mucho más altos que estudios previos basados en PVA-KOH. Los valores de conductividad respecto a la temperatura siguen un comportamiento tipo Arrhenius y aumentan con el incremento de VAVTD alcanzando un máximo de 0.019 S cm^{-1} a temperatura ambiente. Los elevados valores de intensidad y conductividad obtenidos por los geles poliméricos permitieron su implementación en baterías de Zn/aire. A una corriente de descarga de -5mA los hidrogeles presentan una capacidad máxima de 165 mAh y 195 mAh para VAVTD/PVA (4: 1) y (5: 1) respectivamente. Los valores obtenidos son significativamente superiores a los 110 mAh obtenidos con hidrogeles de PVA-KOH.

Palabras clave: PVA, KOH, Electrolito polimérico en gel, baterías, Zn/aire

ABSTRACT

The synthesis of a polymeric gel formed by Poly (Vinyl Alcohol) (PVA) and different proportions of the ter-polymer composed of vinyl acetate, butyl acrylate, and vinyl neodecanoate (VAVTD) was carried out. The gels were doped with Potassium Hydroxide (KOH) by immersing the polymer in a 12M KOH solution for 24 hours, for its subsequent characterization by different spectroscopic, thermal, and electrochemical techniques. X-ray diffraction tests showed a reduction in the polymer crystallinity after being immersed in KOH. Similarly, the cyclic voltammetry test showed that the higher the VAVTD ratio, the current intensities achieved increase, reaching a maximum of 310 mA with a VAVTD / PVA (4:1) membrane. These intensity values obtained are higher than those obtained by previous studies based on PVA-KOH hydrogels. The conductivity values vs temperature follows an Arrhenius-type behavior and increase with increasing VAVTD content with a maximum of 0.019 S · cm^{-1} at room temperature. The high intensity and conductivity values obtained by the polymeric gels allowed their implementation in Zn / air batteries. At a discharge current of -5mA hydrogels have a maximum capacity of 165 mAh and 195 mAh for VAVTD / PVA (4: 1) and (5: 1) respectively. The values obtained are significantly higher than the 110 mAh obtained with PVA-KOH hydrogels.

Keywords: PVA, KOH, GPEs, batteries, Zn / air

TABLE OF CONTENTS

LIST OF FIGURES

LIST OF TABLES

1. INTRODUCTION

In recent decades fossil fuels undoubtedly had the title of humanity's greatest energy source. Despite being a non-renewable energy source, whose combustion generates a large number of toxic pollutants for the environment. Generating a constant concern in the environmental, ecological, social, and economic panorama for the following decades. That is why the search for clean and renewable energy with a low carbon footprint such as solar, wind, geothermal, and hydroelectric energy has become an attractive research topic. However, the variability presented by these energy sources, such as location, season, and climates, together with their often noncoincidence with energy demand, has severely limited their application. To overcome this barrier, energy storage and conversion technologies have received a great deal of attention from commercial companies and national governments[1].

One of the great drivers of these changes is the automotive industry, with the development of electric vehicles, which seeks to reduce its products' carbon footprint. This objective can be carried out by the development of portable batteries with a high energy (tens of kWh) capacity, a long service life, capacity of handle a high power (up to a hundred kW)[2], together with low production costs and reasonable recycling potential.

This growing market has not gone unnoticed, raising the interest of several global actors, such as the case of the European Union where its representative Maroš Šefčovič, vice-president responsible for the Energy Union in the framework of the European Week of Cities and Regions celebrated in 2018, said[3]:

"Regions are the living labs of our industrial policy. It is therefore excellent to see that the European Battery Alliance is now attracting those set to embrace this modernization opportunity and join up with their strengths and capabilities. These interregional partnerships will play a crucial part in building a competitive, innovative and sustainable battery value chain in Europe, to capture a market that could grow to €250 billion annually by 2025 onwards. In the run to the first anniversary of the EU Battery Alliance next week, we will be showcasing that the EU has what it takes to become a global leader here."

Thus, large corporations such as the PSA Group, Renault, and the French battery manufacturer SAFT have joined this initiative of the European Union, obtaining significant capital injections[4].

On the other hand, digitization and technology currently play an essential role in human life. This tendency is reflected in a greater demand for electronic devices such as cell phones, tablets, laptops, and digital cameras. The pandemic caused by the coronavirus (COVID-19) has reflected the essential need of virtual technologies to ensure the proper functioning of society. Thus, the productive sector has been forced to use the telework modality, increasing society's technological dependence. Likewise, the provisions issued by the World Health Organization (WHO) to control this pandemic encourage social distancing.[5] For this and many other reasons, all of the more significant economies have greatly promoted online shopping, teleworking, distance training, remote healthcare, online supply chains, along with other types of goods and services.

All the above has forced companies to increasingly improve their devices' characteristics to meet consumers' demands and needs. That is why a new generation of electrochemical capacitors and batteries is necessary to face future challenges.

At present, there is a great variety of electrochemical systems used in battery design, among which we can name: Zn / MnO_2, Zn / air, Ni / Cd, Ni / MH, and the most used Li-ion. Each of these systems has a specific market niche depending on the needs and required specifications. However, the current high technological demand has driven the development of new energy storage sources, which has to provide higher energy and power values as well as an elevated number of charge/discharge cycles. Prioritizing a decrease in volume and total weights along with an increase in the device security[6].

That is why the Laboratory of Materials for the Production and Storage of Energy of the Polytechnic University of Cartagena (MAPA) has focused its research line on the improvement of storage devices[6,7]. Among them, Metal/air batteries have aroused great interest due to the high specific energies they can supply. Nowadays, only the Zn/air batteries are commercially available.

The present work has focused on the development of a main component in the batteries field, a new hydrogel for its subsequent application as the polymer electrolyte in Zn/air batteries. The results obtained are compared with the literature, for which an overview of the recent innovations in the batteries field is presented.

2. BACKGROUND

2.1. Electrochemical Cells

The electrochemical cell is a device that uses spontaneous chemical reactions to produce electricity or uses electricity to generate non-spontaneous reactions. This process is of utmost importance for electrochemistry and the industry in general since battery operation is based on it. There are two types of electrochemical cells; galvanic cell, also called a voltaic cell, and electrolytic cell, their similarities and differences are listed in Table 1 extracted form Inzelt, G. 2015[8].

Table 1 Comparison between galvanic cell and electrolytic cell

Galvanic Cell	Electrolytic cell
Use spontaneous chemical reaction (Gibbs free energy $\Delta G < 0$) to generate electricity	Use electricity to generate non-spontaneous reaction (Gibbs free energy $\Delta G > 0$).
The electric potential difference (Electrode potential) generated is positive.	The electric potential difference (Electrode potential) generated is negative.
Electrons provided by the oxidized species go through the anode to cathode.	Electrons are supplied by an external source.
Reduction occurs at the cathode while oxidation occurs at the anode.	Reduction occurs at the cathode while oxidation occurs at the anode.
Anode is the negative pole and cathode is the positive pole.	Cathode is the negative pole and anode is the positive pole.

A typical electrochemical cell owns at least two electrodes (cathode and anode) in contact with an ionic conductor (electrolyte) and optionally a separator Figure 1.
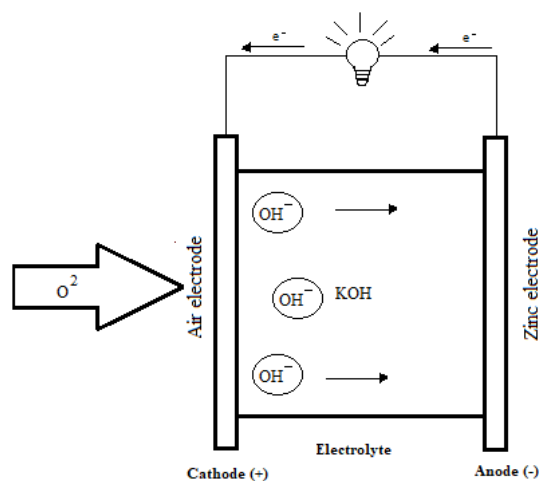
Figure 1 Simplified diagram of a Zinc/air battery.

Since its commercial debut in 1991, lithium-ion batteries have become the most widely accepted electrochemical energy storage globally. However, its insufficient specific energy of ~250 Wh kg^{-1}, which is considerably less than the gasoline's practical value[9], makes them unlikely candidates to fulfill the market necessities. On the other hand, metal/air batteries have specific energy several times higher than the best Li-ion battery[10] which is why they have attracted attention in recent years.

The principle behind metal/air batteries is a redox reaction between the metal in the anode and the environmental oxygen in the porous cathode. One of these batteries' main advantages is the open-cell structure that facilitates a continuous oxygen entry from the air, which translates into a much higher theoretical specific energy[11]. There is a wide variety of metals that can be used as an anode for metal/air batteries, among which we can mention Li, Fe, Mg, Al, Zn, Na, and K. However, the most investigated and promising metals are Li and Zn[12]. Li/air batteries have a high theoretical specific energy of ~11500 Wh kg^{-1}. However, their development has been limited by safety problems due to the high Li reactivity and the high value of commercial Li, which is around ≈60 USD lb^{-1} and the limited access to natural reserves of this material located mostly in Australia and Chile[13].

On the other hand, Zn/air batteries have a lower theoretical specific energy than Li/air batteries (~1350 Wh kg^{-1}). However, it is still four times higher than commercial Li-ion batteries. Among Zn's benefits, we can refer to: Less reactivity contrasted with Li, which generates greater customer security; Zn is the fourth most abundant element in the earth's crust, which is around 300 times more than Li[14]. This abundance generates a lower material cost (≈0.9 USD lb^{-1}) than Li. Moreover, Zn batteries can use aqueous electrolytes

which are cheaper, have higher conductivity values and are environmentally friendly. These benefits provide a considerable advantage over other metal/air batteries.

2.2. Zinc/air batteries

The first primary Zn/air battery was designed by Maiche in 1878 using a silver wire as the air electrode[10]. Subsequent studies resulted in developing an electrode based on black carbon and nickel. Its commercial applications have been limited to seismic telemetry, railway signaling, navigation buoys, and headphones due to its limited recharging capacity. However, market requirements have encouraged companies such as EOS Energy Storage, Fluidic Energy, and ZincNyx Energy Solutions to focus on research to overcome recharge problems[15].

A Zn/air battery is composed of a Zn electrode, a separation membrane, an electrolyte, and an air electrode. Electricity is generated from a redox reaction between Zn and air[16].

Electrodes are materials with high electrical conductivity, usually solids such as zinc, carbon, copper, or iron. The oxidation-reduction reactions take place on its surface and it serves as a connector for the electrons to be transported through the external circuit.

According to Inzelt et al. [8] There are several ways to classify the electrodes among which we can name:

- Depending on the process carried out, the electron, where the reduction takes place, is called the cathode, and the one where the oxidation occurs is called the anode.
- Depending on the functional grouping, they are divided into working electrode also called indicator electrode, reference electrode, and counter electrode. Batteries do not have a reference electrode.

2.2.1. Zinc electrode (anode)

Zinc is a bluish-gray element. Its principal characteristics are an atomic number and weight of 30 and 65.38 u, respectively, a density of 7.14 g cm^{-3}, electrical resistivity of 6.16 $u\Omega$cm^{-1}, and a melting point of 419.5 °C. The standard electrode potential is - 0.76 V in acidic medium and - 1.29 V in alkaline medium. The equilibrium potential of a Zn/air battery is 1.65 V. However, practical working voltages are usually between 1.2 V due to

internal battery losses resulting from activation, ohmic polarization and concentration loss[17].

During the discharge process in alkaline medium, Zn anode is oxidized to Zn^{2+}, which reacts with the hydroxyl ions to form $Zn(OH)_4^{2-}$. However, when $Zn(OH)_4^{2-}$ concentration reaches a saturation point, this specie precipitate forming ZnO. The most accepted anodic electrochemical reactions in alkaline electrolytes are the following[11]:

$$Zn \rightarrow Zn^{2+} + 2e^- \qquad (1)$$

$$Zn^{2+} + 4OH^- \rightarrow Zn(OH)_4^{2-} \qquad (2)$$

$$Zn(OH)_4^{2-} \rightarrow ZnO + H_2O + 2OH^- \qquad (3)$$
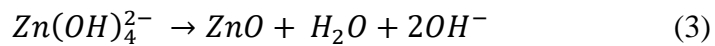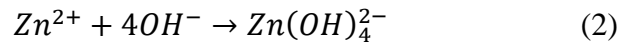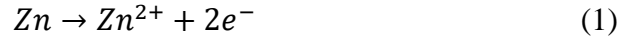
To improve the performance of Zn electrodes, several investigations as the explained below have been proposed[15]:

- **High surface area:** An increase in the surface area of the electrode translates into a lower overpotential for Zn deposition which limits the formation of dendrites that cause short circuits during charging. However, the increased area has been shown to be related to self-discharge when the battery is not operating.
- **Polymeric Binders:** These binders are added to the Zn powder to increase mechanical stability. However, mostly polymers are naturally non-conductive, this generates greater internal resistance in the electrode.
- **Carbon-Based Electrode Additives:** The formation of ZnO during discharge increases the electrode's internal resistance, so carbon-based additives are widely used to improve conductivity and improve chemical resistance in alkaline environments.

2.2.2. Air electrode (cathode)

There are three elemental components in an air electrode: current collector, gas diffusion layer, and the active catalyst layer[18]. Figure 2 graphically shows a structure of an air electrode and its components.

As a general rule, the gas diffusion layer is in contact with the free air and is generally composed of porous carbon materials. Its principal function is to act as a channel for oxygen to enter the battery, giving way to the reaction. Since oxygen is an element with

low solubility and diffusivity, it must have a high surface area, porous structure, and be hydrophobic to prevent electrolyte leakage into the environment.

The current collector is usually a conductive mesh, nickel foam and stainless steel are generally used, and it is located between the other two layers. The active catalyst layer covers the surface between the current collector and the electrolyte, and this is where the oxygen reduction reaction (ORR) takes place. The most active electrocatalysts are made of noble metals and alloys, especially platinum and iridium/ruthenium[19]. Due to the high cost of these materials, noble metals application has been limited and alternative materials such as MnO_2-based catalysts has been sought. A clear example is the Duracell hearing aid batteries that use MnO_2[14].
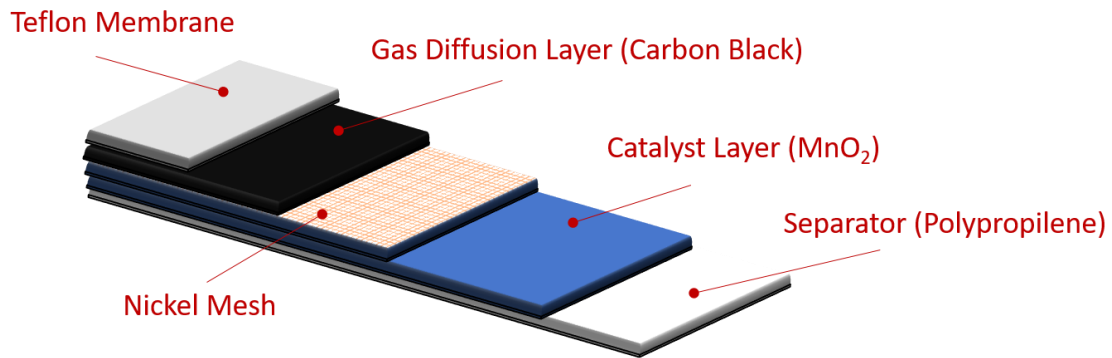
Figure 2 Diagram of a gas diffusion electrode and its different components. [20]

ORR is an electrocatalytic oxygen reaction that occurs during discharge and it can be occurred by a simple (implying 4 e⁻) or a two-step mechanism. For a 4e⁻ mechanism, the most accepted reaction is:

$$O_2 + 2H_2O + 4e^- \rightarrow 4OH^- \tag{4}$$
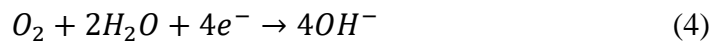
In rechargeable batteries air electrodes allows ORR during discharge process and oxygen evolution reaction (OER) in the charging process. These electrodes are called bifunctional electrodes[21]. The most accepted reactions for OER are the following[12]:

$$OH^- + * \rightarrow OH^* + e^- \tag{5}$$

$$OH^* + OH^- \rightarrow O^* + H_2O + e^- \tag{6}$$

$$O^* + O^* \rightarrow O_2 \tag{7}$$
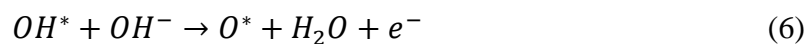
2.2.3. Electrolyte

The electrolyte is in charge of connecting the electrodes, and its main function is to act as a medium for the ions flow between electrodes. An alkaline electrolyte is typically used in Zn/air batteries.

The criteria for a good electrolyte include a) a good dissociation of the salt without the formation of ion aggregation or ion pairs; b) high thermal, mechanical, and chemical resistance; c) good interfacial contact with two electrodes; d) high ionic conductivity[22].

Zn can react violently with acid solutions that is why potassium hydroxide (KOH) and sodium hydroxide (NaOH) are generally used as electrolyte. While, KOH has a greater acceptance due to its higher Zn salts solubility, better oxygen diffusion coefficient, and lower viscosity. Also, the ionic conductivity of K^+ (73.5 Ω^{-1} cm^2 $equiv^{-1}$) is better than Na^+ (50.11 5 Ω^{-1} cm^2 $equiv^{-1}$). The concentration of KOH plays an important role in the battery properties, at a higher concentration the anode corrosion is reduced, it delays the deposition of ZnO, increases the ionic conductivity and shifts the redox potential of the Zn^{2+}/ Zn pair towards more negative values[14].

However, an excessively high concentration of KOH increases the viscosity of the electrolyte which decreases the transfer rate of hydroxyl ions. In addition, lower concentrations of KOH shown greater charge retention and useful battery life, as well as less dendrites growth. Taking these factors into consideration, the most used concentrations in batteries range between 6M and 8M.

2.3. Ionic Conductivity

Ionic conductivity (σ) is a measure to denote the tendency of a substance to favor the movement of an ion from one place to another. This measure is very important for its application in electrochemistry. In batteries development, the ionic conductivity of the electrolyte plays a crucial role in the enhancement of the device performance[23].

In the present work the ionic conductivity was calculated with the following equation:

$$\sigma = \frac{1}{R_b} * \frac{L}{A} \tag{8}$$

Where:

σ Ionic conductivity in S·cm^{-1}

L   Membrane thickness in cm

A   Contact surface of the electrode with the membrane, in cm^2

R_b Resistance of the polymeric membrane electrolyte, in ohms (Ω)

The dependence of temperature presented by conductivity can be explained by the Arrhenius model Ec. (10). Here, E_a is the activation energy; σ_o represents the pre-exponential factor; K represents the general gas constant; T represents the absolute temperature. The plot ($\ln \sigma \; vs \; \frac{1000}{T} \; (K^{-1})$) is used to present Arrhenius dependence.

$$\sigma = \sigma_o \exp\left(\frac{-E_a}{KT}\right) \qquad (9)$$

Vogel-Tammann-Fulcher (VTF) [24] theory and William-Landel-Ferry (WLF) [25] theory are also used to explain ions migration however they will not be used in this work.

2.4. Polymeric electrolytes (PEs)

In 1973 Fenton et al. began their research on polymeric electrolytes (PEs) by taking poly (ethylene oxide) (PEO) as a polymeric host along with sodium and potassium salts [26]. The electrical conductivity of the PEs generated by Fenton based on potassium thiocyanate presented a high-temperature sensitivity as well as a decrease in crystallinity. However, the importance of these electrolytes was highlighted in the 1980s with the contributions of (Armand, 1986; MacCallum and Vincent, 1987,1989; Ratner and Shriver, 1988)[27]. In recent years the development of new PEs has received increasing attention.

For many years, liquid electrolytes have played an essential role in the electrochemistry of energy storage, providing high ionic conductivity, good contact with electrodes, and low cost. However, its use has been shown to have risks, among which we must highlight[28]:

- In lithium or zinc batteries with liquid electrolytes, the formation of a dendrite in the electrolyte occurs, generated by unequal currents in the charging processes. This dendrite can cause a short circuit that reduces the battery's maximum charge/discharge cycles. [25]
- The problem of hermetic sealing generates a risk of toxic gas leaks as well as a risk of combustion when working with organic electrolytes.

- In alkaline batteries with Zn electrodes, corrosion and subsequent dissolution of the anode in contact with potassium hydroxide (KOH) can be generated.
- Bumps can cause a rupture, creating the possibility of a leak of the battery's internal liquid. The corrosive attribute of liquids poses a risk to the user.

PEs are generally defined as membranes with transport properties like common liquid ionic solutions, typically composed for the dissolution of salts in a polymer host matrix. Among the most relevant properties of PEs, we can mention their transparency, flexibility, wide electrochemical windows, high ionic conductivity, solvent-free, and ease of processing. [27]

Polymers have two phases, one crystalline and the other amorphous, this ratio varies depending on each polymer. However, ion transport has been shown to occur mainly in the amorphous zone, in the same way, PEs with a high viscosity generates high ionic conductivities[29].

This solvent-free system is considered an evolution from polymer, liquid ionic conductor, and solid-state ionic conductor. It is widely applied in electrochemical devices such as rechargeable batteries, fuel cells, analog memory devices, etc. Moreover, they also exhibit attractive prospects for electronic vehicles (EV) and aviation technology. In principle, a polymeric electrolyte battery can be generated by trapping the electrolyte between the anode and the cathode.

Based on their source and origin, PEs are divided into i) natural group, among which we can name chitosan, rice, and corn starch, and ii) synthetic group. However, the most

widely used division is according to its physical state and composition, as it is shown in Figure 3.
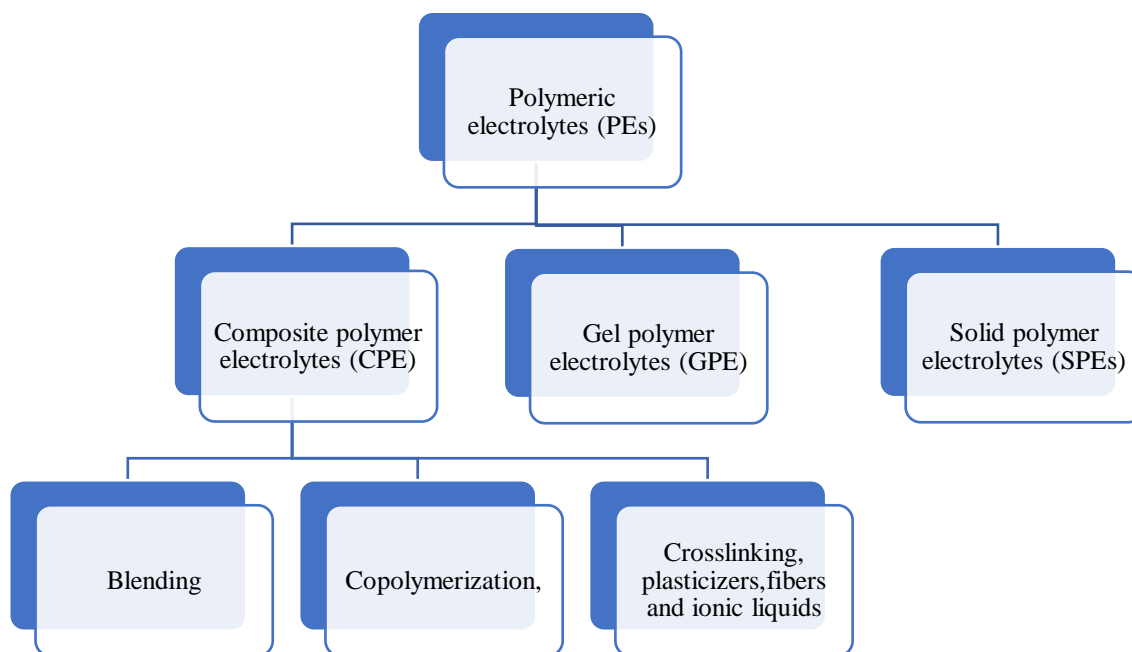
Figure 3 Different types of PE based on their physical condition.

2.5. Solid polymer electrolytes (SPEs)

The first battery that used a solid-state electrolyte was generated in 1979 by Armand et al. based on Polyethylene Oxide (PEO) as a polymer host and a lithium salt complex [30]. The advantages exhibited by the SPEs compared to the classic liquid electrolytes, among which we can mention the ability to generate thin films, good electrode/electrolyte contact, and good mechanical properties provided an increasing interest in developing rechargeable solid electrolyte batteries.

Several investigations have been carried out with different polymers including, polypropylene oxide (PPO), poly [bis (methoxy-ethoxy-ethoxy) phosphazene] (MEEP), polysiloxane (PSI), etc., all of them amorphous at room temperature. However, the most promising and researched one for its application in SPEs is (PEO).

Despite the interesting properties of SPEs, its application has been limited due to the low values of ionic conductivity at room temperature presented ($\sim10^{-4}$ S cm^{-1} at 25 $^{\circ}$C). Some of the advances in SPEs are presented in Table 2[31].

Table 2 Advances in SPEs based on combination of polymer host, electrolytic salt and its ionic conductivity at room temperature.

Polymer host	Electrolytic salt	Solvent	Ionic conductivity (S cm^{-1})	References
PVA	Mg (NO$_3$)	Triply distilled water	7.36×10^{-7}	32
PEO-PMMA	LiClO$_4$	NMP	1.59×10^{-5}	33
PVC-PEMA	LiPF$_6$	THF	10^{-3}	34
PEO	LiClO$_4$		1.2×10^{-3}	35
PMMA	LiClO$_4$	-----	7.04×10^{-3}	36
PVB	LiClO$_4$	------	2.15×10^{-6}	37
PAN-PVA	LiClO$_4$	EC/DMC	2.5×10^{-4}	38

2.6. Composite polymer electrolytes (CPEs)

To overcome the disadvantages and limitations presented by the PEs, CPEs have been developed. Among the techniques used for this purpose, we can find polymer blending, copolymerization, crosslinking, plasticizers, fibers, and ionic liquids. [39]

2.6.1. Polymer blending

In this process, two or more polymers with or without chemical bonds between them are combined to generate a new polymer matrix with desired properties. The polymers may belong to the same chemical family (low, high, or ultra-high molecular weight) where they are called homologs or may belong to entirely different families where they are called heterogeneous. [27]

Juan Shi, Yifu Yang, and Huixia Shao in 2018 examined a polymer blend of PEO/ PMMA/P(VDF-HFP) and it was tested in secondary lithium batteries. The results showed that this blend could increase the amorphous structure of the PEs, also increase their porosity and the amount of liquid electrolyte that it can retain. The study calculated the ionic conductivity values presented by pure PVDF-HFP GPEs and the blend GPEs as 0.25 mS cm^{-1} and 0.81 mS cm^{-1} at 25 ° C respectively. These results are attributed to the increase in the amorphous zone, which facilitates the transport of Li$^+$ ions, while the increase in liquid electrolyte provides a greater number of Li$^+$ ions[40].

2.5.2. Copolymerization

Copolymerization is defined as the simultaneous polymerization of two or more different monomers. Its main objective is to obtain polymers with a balance of properties favorable for commercial applications[41]. There is an almost unlimited range of possible combinations and four basic copolymer structures: random, alternating, block, and graft. Random copolymers have a random monomer distribution along the polymer chain. Block copolymers have uninterrupted sequences of each monomer. Figure 4 a) represents a simplified copolymerization of monomers A and B generating the block copolymer A-B. Alternating copolymers have two monomer units alternately one before the other. Graft copolymers in general are branched copolymers where the chain is made up of one monomer and the branches of another. Figure 4 b) represents a simplified formation of the poly (vinyl alcohol-co-ethylene) from its starting monomers vinyl acetate and ethylene.
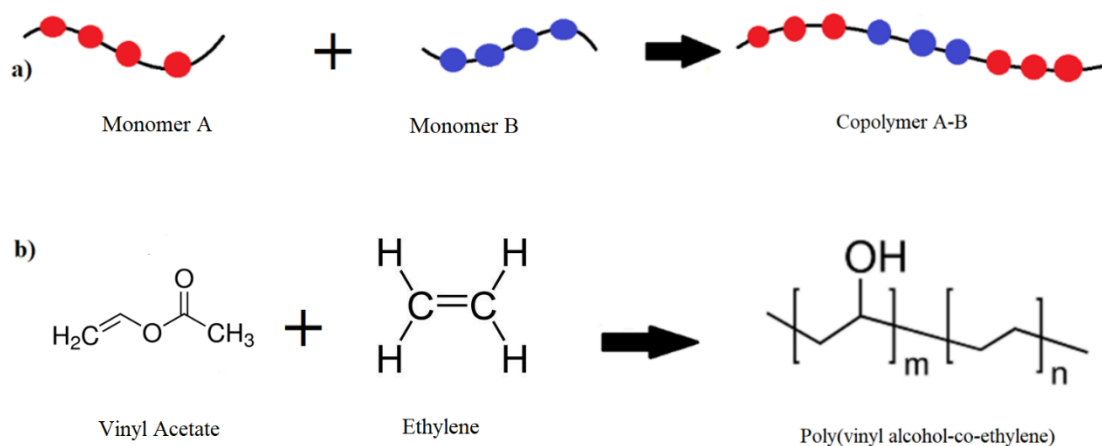
Figure 4 a) Schematic representation of a copolymerization of the monomers A and B. b) Simplified copolymerization of Vinyl Acetate and Ethylene.

2.7. Gel polymer electrolytes (GPE)

GPEs are also known as plasticized PEs, and they are neither liquid nor solid. However, they have characteristics of both. Conserving the cohesive properties of solids as well as the ion diffusive properties of liquids[42]. The first approaches towards the generation of gel polymer electrolytes were given in 1975 by G. Feuillade and Perche. They described the formation of a quasi-solid gel electrolyte generated from the combination of a non-aqueous saline solution with a polymer and its application in a lithium cell [43]. The GPE resulting had high electrical conductivity and could be used as a separator between battery electrodes. Hydrogels are a type of GPE used primarily on flexible supercapacitors. The

main advantages of hydrogels are self-healing, shape memory, availability of use aqueous-based electrolytes, eco-friendly and resistance to cold and heat[44].

GPEs can be prepared by cast method, the polymer chosen as the host is dissolved in a suitable solvent, and then a solution of an alkali metal salt is added. The mixture is stirred and then it is allowed to evaporate either at room temperature or on a hot plate to form a thin-film. Once most of the solvent has evaporated, the salt will be trapped in the polymer matrix.

GPEs present attractive properties such as high ionic conductivity compared with solid polymer electrolyte ($\sim 10^{-3}$ S cm^{-1} at 25 ^{o}C), low volatility, good operation safety, light weight, wide electrochemical window, high energy density, good volumetric stability, non-combustible reaction products at the electrode surface and its easy adaptability, elasticity and flexibility to cover the desired shape. These properties make them great candidates for use in charge storage devices such as batteries, supercapacitors, fuel cells, etc. [27]. Compared with liquid electrolytes, GPEs eliminate the leakage hazards, limiting an internal short circuit's risk, increasing the useful life sacrificing some ionic conductivity.

To obtain a high salt dissociation, it is important to use a solvent with a high dielectric constant ($\varepsilon > 15$), organic solvents are frequently used for this purpose among the most used we can mention: ethylene carbonate (EC), propylene carbonate (PC), diethyl carbonate (DEC), dimethyl carbonate (DMC), dimethylformamide (DMF), dimethyl sulphoxide, ethyl methyl carbonate, and tetrahydrofuran [22].Table 3 presents advances in GPEs field[31].

Despite the many advantages that GPEs possess, there are still several limitations to their general application. Among which can be mentioned the need to apply a liquid electrolyte solution to the polymer, which reduces the mechanical and thermal properties. Similarly, the formation of GPEs presents slow evaporation together with a poor interaction between the interfacial activity with lithium electrodes [45]. The term hydrogel used in this work applies when the polymer gel has been manufactured in an aqueous medium.

Table 3 Advances in GPEs based on combination of polymer host, electrolytic salt and its ionic conductivity at room temperature

Polymer host	Electrolytic salt	Solvent	Ionic conductivity $(S\ cm^{-1})$	References
PVA	NH_4SCN	DMSO	2.58×10^{-4}	46
PVB	$LiPF_6$	-----	4.09×10^{-4}	47
P(EO-co-PO)	$LiPF_6$	DMF + distilled water	2.80×10^{-3}	48
PEMA	$LiBF_4$-EC/EMC/PC	THF	5.80×10^{-4}	49
PVdF-HFP	Urea/PVP	DMF	2.823×10^{-3}	50
PVA	KOH	Distilled water	7.92×10^{-3}	20
PVdF-HFP	$ZnTf_2$ and 1-Ethyl-3-methylimidazolium bis(trifluoromethylsulfonyl)imide as ionic liquid	n-methyl-2-pyrrolidone	7.07×10^{-3}	51

2.8. Polymer host

To prepare a polymeric electrolyte it is necessary to have the presence of at least one polymeric host which takes the role of base and support for the PE. Some of the commonly used polymers are poly (vinyl chloride) (PVC), poly (vinyl alcohol) (PVA), poly(acrylic acid) (PAA), PEO, poly (acrylonitrile) (PAN), poly (vinylidene fluoride) (PVdF), poly (ethyl methacrylate) (PEMA), poly (methyl methacrylate) (PMMA), poly (vinylidene fluoride-hexafluoropropylene) (PVdF-HFP), chitosan etc[39]. According to Michel Armand [52] and Wolfgang Meyer [53] the criteria to evaluate a host polymer are:

a) **The segmental motion of polymer chain:** The ions are proposed to form a complex with the polymer chain, decreasing their mobility and forming a dependency with the polymer segments' movement. For this reason, the ionic movement between the complexation sites is assisted by the segmental movement.

b) **Dielectric constant:** The dissolution of inorganic salts in a polymer matrix is favored when the salt's reticular energy is low, and the host polymer's dielectric constant is high.

c) **Functional Groups:** The presence of functional groups can hinder ionic complexes' formation. Such is the case of poly (propylene oxide) (PPO) which, since it has a methyl group, hinders the formation of the complex compared to Polyethylene glycol (PEO), which does not have the methyl group. On the other hand, functional groups such as (-O- and -S-) facilitates the dissociation of lithium salts from lithium ions. Likewise, the presence of a large pendant group gives Poly (ethyl methacrylate) greater flexibility and adaptability for the formation of PEs.

d) **Glass transition temperature (Tg):** The segmental motion occurs at temperatures above Tg for that reason polymers with low Tg have better ionic conduction properties at room temperature.

e) **Electrochemical stability window:** It is defined as the difference between the potentials of the oxidation and the reduction reaction. An electrolyte should be inert to both electrodes it means that the reduction potential should be lower than the metal employed in the anode and oxidation potential should be higher than the cathode metal.

f) **High degradation temperature:** The polymer must have a high enough degradation temperature to withstand the manufacturing processes of electronic devices as well as the operating conditions.

g) **Cost:** In practice, the polymer's price plays a fundamental role. It should not be expensive since it makes the final less competitive in the market. Additionally, it is important to consider the price of recycling after the useful life of the product.

2.8.1. Poly (vinyl alcohol) (PVA)

PVA is a water-soluble polyhydroxy polymer that contains mainly 1,3-diol units and 1-2 % of 1,2 -diol when it's polymerized by hydrolysis. Its structure is presented in Figure 5. Its chemical formula is (C_2H_4O) n, where n indicates the repeating unit of a polymer chain. Due to the absence of a vinyl alcohol monomer, the production of PVA is carried out by indirect methods. The most commonly used method is the hydrolysis of the poly (vinyl acetate) polymerized in methanol. The characteristics of PVA
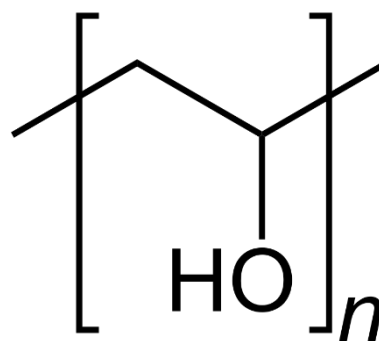

Figure 5 Structure of Poly (vinyl alcohol) (PVA).

will be mainly influenced by its degrees of polymerization and the residual content of acetyl groups [54].

Globally, the main applications of PVA are in the textile, paper, and adhesive industries. However, its high mechanical resistance characteristics, good thermal stability, hydrophilic behavior, biodegradability, non-toxicity, easy preparation, and low cost have allowed PVA to be implemented in fields such as medicine and electrochemistry[55].

2.8.2. Poly vinyl acetate emulsions

Over the years, polyvinyl acetate emulsions have become an attractive product for the market due to their industrial applications (interior and exterior architectural coatings, adhesives, and paints) generated by the films' physical characteristics availability, and low cost[56]. Furthermore, its ability to copolymerize has allowed the creation of various latexes with innovative properties. One of the most used co-monomers in latex preparation is butyl acrylate (BuA), particularly the copolymer generated with a BuA concentration between 15 -25 wt% is widely used in the architectural coatings industry[57]. However, due to the great difference between the reactivity ratios, large chains rich in VAc are formed, contributing to limited alkaline stability. Implementing the vinyl neodecanoate co-monomer (VeoVa10) with a similar reactivity relationship and a branched structure protects the VAc[58]. The low production cost of this polymer together with its high amorphousness has made it a candidate to be considered in electrochemistry.

3. OBJETIVES

3.1. General

- To develop a polymer host based on VAVTD-PVA blends for its implementation in Zn/air batteries.

3.2. Specific

- To synthesize a new GPEs varying the VAVTD concentration and keeping the PVA concentration constant.

- To compare the impact of VAVTD - PVA GPEs with pure PVA GPEs.

- To characterize and analyze the structural, thermal, and electrochemical behavior of the VAVTD – PVA submerged in KOH GPEs.

- To identify if the implementation of VAVTD in GPE is a viable alternative in the development of Zn/air batteries.
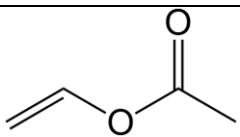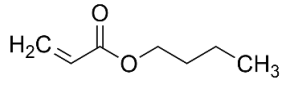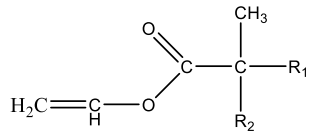
4. MEHODOLOGY

4.1. Reagents and Materials

a) Poly (vinyl alcohol) (PVA), MOWIOL 18-88 (MW 130.000), obtained from Sigma -Aldrich.

b) Poly (vinyl acetate)-co-Poly (butyl acrylate)-co-Poly (vinyl tert-decanoato) (VAVTD)

VAVTD terpolymer was provided by the PhD. Antonio Diaz Barrios, and was previously reported in the article *"In situ synthesis and long-term stabilization of nanosilver in poly(vinyl acetate-co-butyl acrylate-co-neodecanoate) matrix for antibacterial applications"*[59]. Vinyl acetate, butyl acrylate, and vinyl tert-decanoate (VeoVa 10) with an initial concentration of 70/15/15 w/w respectively were the starting monomers of the emulsion polymerization using ammonium persulfate and tert-butyl hydroperoxide as radical initiators, Table 4 presents the structure of the starting monomers. The reaction temperature was 353 K, and the reaction time was 5 hours.

Table 4 Structure of the starting monomers and the weight percentage of the VAVTD copolymer

Monomer	Structure	Glass Transition Temperature (Homo-polymer)	Water Solubility at 20 C (g / 100g)	Initial monomer concentration w/w %
Vinyl acetate		35 C	2.5	70
Butyl acrylate		-53 C	0.16	15
VeoVa 10	$R_2 + R_1 = 7$ Carbon atoms	-3 C	0.001	15

As can be appreciated in Figure 6. The emulsion copolymer obtained has a milky white coloration with a bluish hue, which according to J. Santiana, can be used as an indicator to confirm that the particle size is in the range of 150 nm to 300 nm[60].

Figure 6. VAVTD copolymer. Taken from Santiana 2017.[60]

   c) Potassium hydroxide (KOH), 85% purity, obtained from Sigma -Aldrich.

   d) Zinc (Zn) powder, 98.7% purity, supplied by Goodfellow.

   e) Air E4B cathode supplied by Electric Fuel Ltd.

   f) Al_2O_3 Polishing Suspension, (1 and 0.05) micron, Buehler.

4.2. Equipment

   a) Potentiostat, Biologic, "VSP" model.

   b) Refrigerated / Heating Circulator, Julabo, "F25-ED" model. Working range from (-28 to +150) ^{0}C.

   c) Hot plate and magnetic stirrer, JP-Selecta, "AGIMATIC-N" model.

   d) Analytical balance, OHAUS, "Pioneer PA114C" model.

   e) Hydraulic press.

   f) Infrared spectrophotometer (FTIR), Thermo "Nicolet 5700" model.

   g) Xray-Diffraction and Scattering "D8 Advance", Cu-Kα detector ($\lambda = 1.5418$ Å).

4.3. Experimental procedure

The study was carried out thanks to cooperation between Yachay Tech University represented by Professor Ph.D. Juan Pablo Tafur and the student Edwin Reyes Jacome while the Polytechnic University of Cartagena (UPCT) was represented by professor Ph.D. Antonio J. Fernández Romero and the Ph.D. Florencio Santos, in the Laboratory of the Group of Advanced Materials for Energy Production and Storage located in the ELDI (Research Laboratory Building) and the Technological Research Support Services (SAIT).

4.3.1. Membrane synthesis

The film preparation was carried out applying the solution casting method. 1 gr of PVA was dissolved in 15 ml of distilled water at 90° C under continuous stirring for two hours until PVA was completely dissolved. When the solution was cold, different amounts of VAVTD (1, 2, 3, 4, 5) gr were added under continuous stirring. The mix was placed in a petri dish and let to cast at room temperature (30° C) for 1 week. When the water was completely removed, a film was obtained. The resulted films were immersed in a KOH solution 12M for 1 day.

4.3.2. Swelling Ratio (SR) determination

To carry out an SR study, it is necessary to determine the initial mass of the membrane to be analyzed, after which the membrane is immersed for 24 h in a 12M KOH solution, and then proceed with a new weighing to determine the final mass. The equation used is the following:

$$SR = 100 \; x \; \frac{m_e - m_d}{m_d} \tag{10}$$

Where m_d and m_e represents the samples weights before and after swelling.

4.3.3. Zinc electrode preparation

The electrodes were prepared according to the following procedure: 1 gram of zinc powder was weighed on the precision balance and was subsequently placed in the hydraulic press at a pressure of 10-ton cm^{-2} using a 12 mm mold to give it the desired shape.

To remove irregularities on the electrode surface, a 1µm and 0.05 µm polishing suspensions is used. Finally, the electrodes were washed with distilled water to remove any polish trace.

4.3.4. Zn /GPE/air Battery formation

1 gr of Zn powder is placed inside a steel capsule as an anode; above it, the GPE is placed. Above the GPE, the Air E4B cathode is placed. Two nickel meshes (1 for each electrode) are placed as collectors in contact with the two electrodes. Finally, the battery is placed on Teflon support to maintain constant contact during the test. Two screws located at each end of the bracket provide stability. Figure 7 presents a scheme of the battery used.
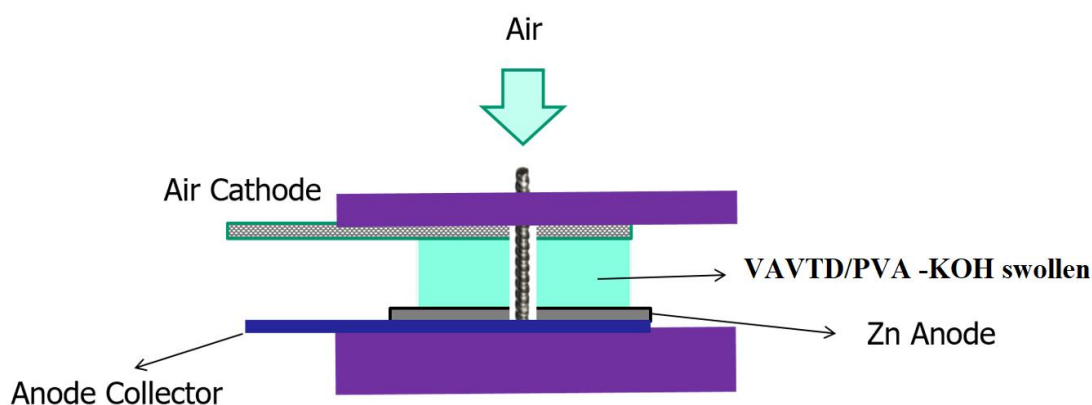
Figure 7 Schematic drawing of Zn/GPE/air battery structure [20]

4.3.5. Ionic conductivity calculation

Potential Electrochemical Impedance Spectroscopy (PEIS) has been used to determine both solid and liquid materials' electrochemical properties. This technique is used in the present work to evaluate the ionic conductivity of the GPEs. All measurements were made under floating potentials, which means that the reference electrode has been connected directly to the counter electrode. The frequency range worked was from 1 MHz to 10 MHz, and the cell configuration used was Pt / GPE / Pt, a 1 cm^2 area Pt electrodes act as blocking electrodes. The sample thickness was measured with a micrometer, and the equipment used was a Potentiostat, Biologic, "VSP" model.

To study the conductivity dependence with respect to temperature, a Julabo F25-D cryothermostat was used, the measurements were made from 5 ºC to 70 ºC with a variation of ±1 ºC. After each temperature drop, the system was stabilized for 45 min

before taking the resistance measurement (R_b). Measurements were made three times, and the average was reported.

4.3.6. Cyclic Voltammetry (CV)

CV study was carried out using a Zn/GPEs/Zn symmetric cell (Figure 8). The scanning speed used was 50 mV/s, in a potential window from -2 V to +2V. The equipment Potentiostat, Biologic, "VSP" model is used for this technique.

Figure 8 Zn / GPE / Zn configuration cell used for CV.

5. RESULTS AND DISCUSSION

5.1. Structural characterization of the Gel Polymer Electrolytes

5.1.1. Swelling Ratio (SR)

Table 5 shows the swelling ratio of the synthesized membranes. The equation used to determine the SR is the following:

$$SR = 100 \; x \; \frac{m_e - m_d}{m_d} \tag{11}$$

Where m_d and m_e represents the samples weights before and after swelling. Pure VAVTD has the highest SR reaching 313,9% of its initial weight, which means that it retains three times its electrolyte weight. On the other hand, PVA presents the lower SR reaching 48,762 %.

Table 5 Swelling ratios for different PVA-VAVTD membranes after their immersion for 24h in KOH 12 M.

VAVTD -PVA	Initial weight /g	Weight after soaking /g	Swelling Ratio /%
1:0	0,023	0,095	313,913
1:1	0,103	0,206	99,515
2:1	0,131	0,282	116,398
3:1	0,139	0,329	137,373
4:1	0,203	0,488	140,275
5:1	0,190	0,505	165,441
0:1	0,065	0,096	48,762

Although VAVTD absorbs a large amount of KOH, its mechanical resistance is greatly affected. The resulting membrane is not kept in a gel state. That is why PVA is added to increase mechanical resistance. PVA previous studies have shown that hydrogels formed by PVA/30ml KOH immersed for 24 hours in 12M KOH reached a SR value of $34 \pm 2\%$[7].
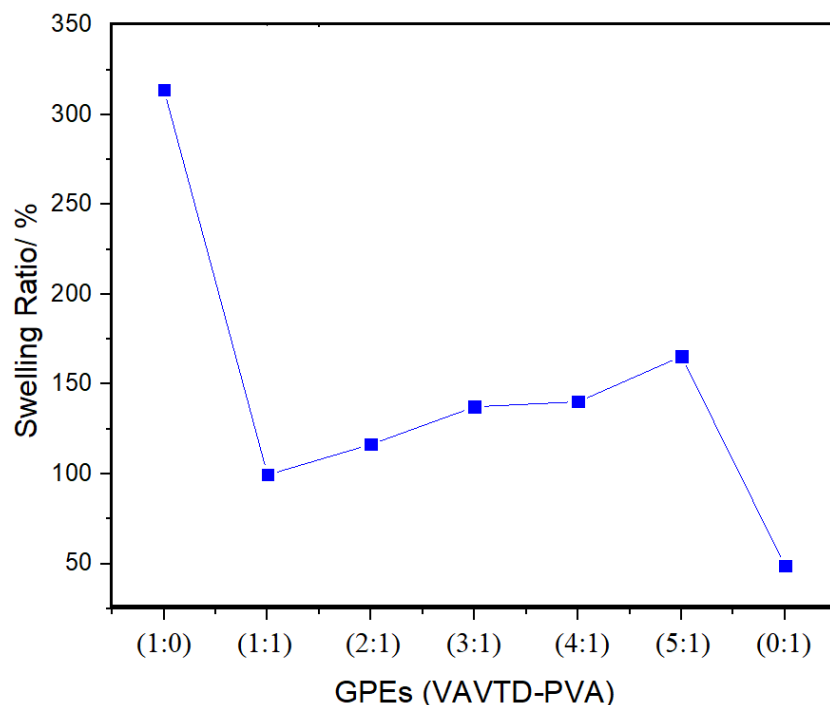
Figure 9 GPEs vs Swelling Ratio (%) Graph

In Figure 9 the relation between the GPEs vs the SR can be observed. When the proportion of VAVTD increases, the SR obtained also increases. When immersed in a thermodynamically compatible solvent (KOH), the solvent will initiate a diffusion process through the polymer chains increasing its amorphousness. The solvent first attacks the amorphous areas of the polymer, so the result SR suggests a lower degree of crystallinity in the VAVTD polymer. Similarly, based on the results, it is objected that PVA has a higher degree of crystallinity. As the solvent penetrates the polymer matrix, its structure changes to a more thermodynamically stable one called "coil".

5.1.2. X-ray diffraction (XRD)

X-ray diffraction is a non-destructive technique used to characterize crystalline materials to obtain information such as unit cell parameters, particle size, atomic position, and quantitative and qualitative assessment of heterogeneous samples.[61]

This technique uses the physical phenomenon of the diffraction of electromagnetic radiation by matter to generate structural information of a crystalline compound. To describe this phenomenon W.L. Bragg, who is considered one of the fathers of diffraction, proposed the following equation:

$$n\lambda = 2\text{d}\sin\theta \tag{12}$$

The analyzed VAVTD sample has 70% vinyl acetate (VA), therefore a diffraction pattern similar to the one presented by polyvinyl acetate (PVAc) can be expected. PVAc have a peak in their diffraction pattern located at $2\Theta = 20^{o}$[62]. In Figure 10 a), we can appreciate that the membrane synthesized with pure VAVTD presents the expected peak at $2\Theta = 20^{o}$ along with a high level of amorphousness compared with pure PVA, this peak is related to the presence of VAc segments long enough to form nano-crystals. On the other hand, pure PVA membranes were fully characterized by different research groups[63,7]. The first peak located at $2\Theta = 20^{o}$ represent a strong crystalline reflection (d=4.46) for a characteristic reflection from (1 0 1) in a monoclinic unit cell[64], a secondary peak at 40.5^{o} can also be observed. The peaks observed are due to the crystallographic planes present in the polymer semi-crystalline structure generated by the interaction between the OH groups present in the PVA backbone chains by H- bonds as can be seen in Figure 11 A) and B).
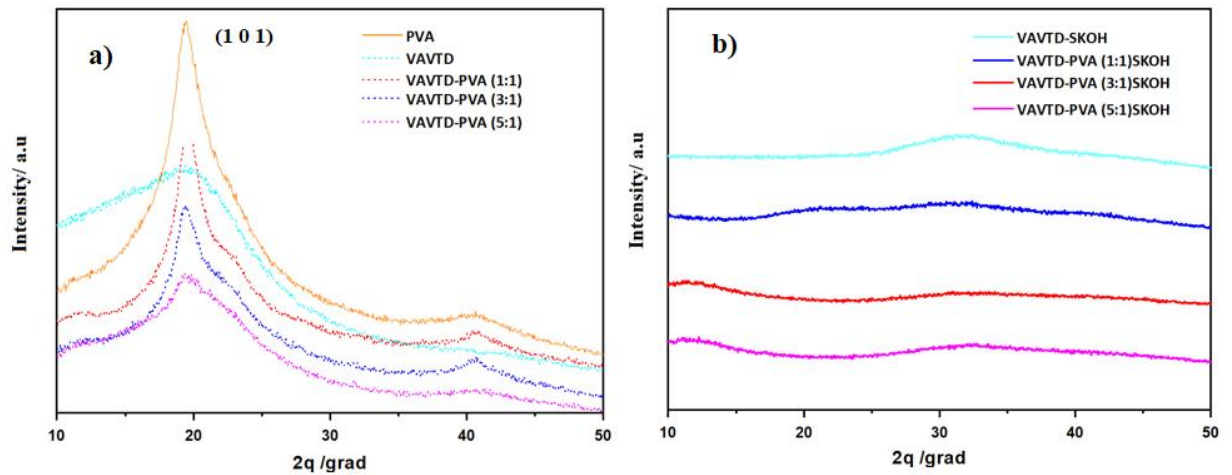
Figure 10 a) X ray diffraction spectra of VAVTD – PVA membranes; b) X ray diffraction spectra of VAVTD – PVA GPEs after been immersed in KOH

With Figure 10 b) when the membranes were immersed in KOH, we can glimpse the following two main characteristics of the GPEs:

1. When PVA and VAVTD were blended, a decrease in the intensity of the characteristic peaks of the polymers is observed, which is associated with a decrease in the degree of crystallinity. When the percentage of VAVTD increases, the intensity of the peaks decreases. The characteristic peaks of PVA can be observed, although with less intensity.

2. The membranes immersed in 12M KOH (SKOH) show a decrease in the intensity of the peaks compared to those that were not immersed, which indicates an increase in the amorphous phase present due to the interaction between KOH, H_2O, and the polymer chains.

Figure 11 C) represents the interaction generated between the polar groups present in PVA and VAVTD with the water molecules and (OH) groups, weakening the attractive forces of the hydrogen bonds generated in the polymer chains[65], this process generates an increase in the amorphous zone of the polymer. The increased amorphous zone leads to an increase in the sample's free volume along with a greater segmental movement. These segmental movements increase allows a greater ion mobility, which is directly related to the GPE conductivity.
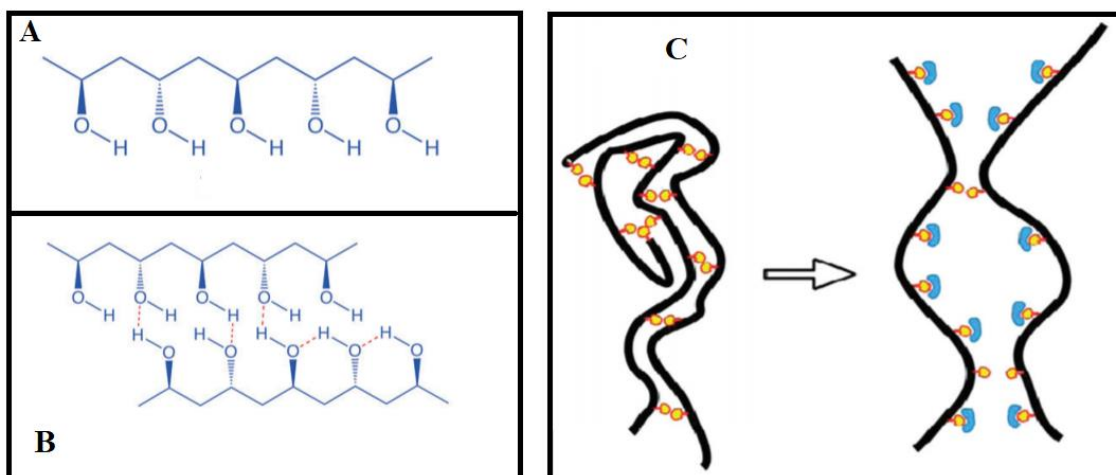
Figure 11 A) Chemical Structure of PVA; B) Hydrogen bonding present in PVA structure[66]; C) Effect of water absorption in polymers proposed by Szakonyi and Zelkó[65].

5.1.3. Fourier Transform Infrared Spectroscopy (FTIR)

Infrared spectroscopy is a widely used technique in characterizing materials. This technique is based on the interaction via exposure of the analyzed molecule to infrared electromagnetic radiation. The frequency ranges typically analyzed are from 4000 to 400 cm^{-1}. The infrared spectrum obtained is used as a "fingerprint" in this way, it is possible to determine the identity, quality, impurities, and existing changes in the sample.[67]

When the molecules absorb infrared radiation, their bonds undergo a molecular vibration which can be stretching and bending. These vibrations are characteristic for each functional group since they appear at a specific wavelength. For this experiment, a Fourier

Transform Infrared Spectroscopy (FT-IR). Attenuated total reflection (ATR) from Thermo "Nicolet 5700" was used.

Figure 12 shows the spectrum FTIR_ATR of the VAVTD-PVA membranes before being immersed in KOH. In the same way, the pure VAVTD and PVA spectra can be observed. Pure PVA presents bands at 1243, 1084, 945 cm^{-1} which correspond to (C-O-C), (C-O), and (C-C-O) groups respectively[68,7]. Thus, it also presents a band at 1732 cm^{-1} which belongs to the (C = O) group associated with the not polymerized acetate groups from the PVA polymerization process, the percentage according to the manufacturer is 12%. On the other hand, VAVTD, like PVA, has the peak at 1732 cm^{-1} associated with (C = O) group; however, its intensity is higher. This is because the components of the VAVTD (VAc, VeoVa 10, BuA) possess a large number of acetate groups [69]. The same happens with the peak located at 1243 cm^{-1} associated with the ether group (C-O-C). The PVA formation process by hydrolysis of the poly (vinyl acetate) eliminates the ether groups, so the peak has little intensity attributed to unpolymerized monomers. While the VAVTD has a high number of ether groups in its chain. The higher the VAVTD concentration in the polymer matrix, the 1732 cm^{-1} and 1243 cm-1 peaks have higher intensities.
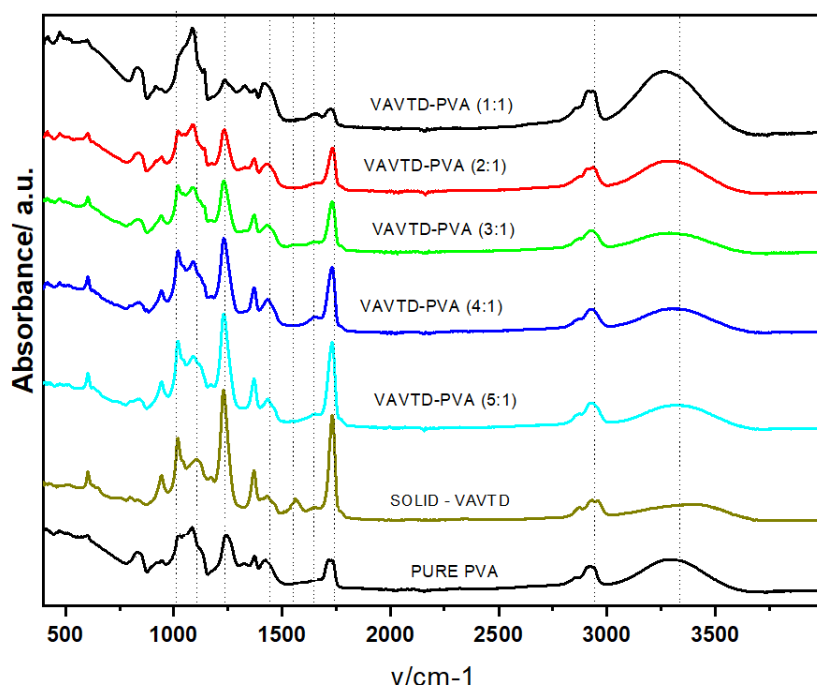

Figure 12 FTIR spectra of VAVTD – PVA membranes before been immersed in KOH.

Figure 13 presents GPEs before and after being immersed in KOH. When comparing the presented spectra, we can observe several differences, among which it is worth highlighting:

- When GPEs are immersed in KOH, we can observe the appearance of a peak located in 1645 cm^{-1} which, according to the authors Almafie et al.[70] and Szymanska et al.[71] represent absorbed water in the sample. Observing this result, we can ensure that water molecules and KOH have penetrated the polymer matrix.

- The disappearance of 945 cm^{-1}, 1243 cm^{-1} bands, and the displacement of 1732 cm^{-1} band, may indicate the hydrolysis of the acetyl groups by the anion OH$^-$ of KOH or by PVA crosslinking. Also previous studies have shown the decrease, displacement or disappearance of C = O groups belonging to acetate groups due to the interaction with KOH[72]. J. Fu et al[73]. and F. Santos et al[7]. reported the disappearance of the peak presented at 1732 cm^{-1} assigned to C = O when GPE is submerged in KOH together with the appearance of a new peak at 1571 cm^{-1} and 1560 cm^{-1} respectively. The authors attribute this behavior to the acetate groups' interaction with K$^+$ cations.

- The region between 3200 to 3550 cm-1 is attributed to the OH groups' stretching vibration. The presence of a very broad and intense peak is associated with concentrated solutions and shows a high degree of association. Similarly, broader peaks and lower frequencies such as those presented by GPEs immersed in KOH are related to an increase in hydrogen bonds'[74]. This indicates the creation of a new hydrogen bridge due to the interaction of water molecules and hydroxyl groups with the polymer chain[7].

Based on those mentioned above, it is proposed that the main interaction takes place between PVA and KOH, forming complexes such as C = O $\cdots$ K$^+$ or CO $\cdot$$\cdots$ K^{+}[7] which have been previously reported in PVA doped with Mg^{2+} or Cd^{2+} salts[75]. This thought finds validity because the 1084 cm^{-1} band assigned to the interaction (C-O) of the PVA decreases when KOH is added.

With the analysis of the infrared spectrum, we can conclude that the water molecules together with KOH penetrate the matrix of the polymer, which generates an interaction between the functional groups (C = O) and (C-O) present in the polymer chain with water, K$^+$ cation and OH$^-$ anion belonged to KOH.

Figure 13 FTIR spectra of VAVTD – PVA GPEs after been immersed in KOH.

5.2. Thermal properties of the Gel Polymer Electrolytes

5.2.1. Thermogravimetric Analysis (TGA)

TGA technique is an analytical technique used to determine the thermal stability and the fraction of volatile compounds present in the sample through the variation in mass produced at a constant variation of temperature. Its usefulness to understand the thermal events that occur when the temperature increases, such as: decomposition, sublimation, reduction, desorption, absorption, etc. [76]. On the other hand, it does not allow to identify processes in which a mass change is not involved, such as fusions or phase transitions.

The equipment used is the Mettler Toledo "TGA / DSC 1HT" thermogravimetric analyzer. The samples analyzed had a mass between 10 to 20 mg and were placed in sealed aluminum pots with a lid. The sampling temperature is from 30 - 700 $^{\circ}$C with a temperature ramp of 10 $^{\circ}$C min^{-1}. The results were evaluated with the STARe Software version 10.0.

Figure 14 compares the thermogravimetric curves of pure VAVTD and VAVTD-PVA membrane (continuous lines) with the VAVTD-PVA GPEs immersed in a KOH solution

(broken lines). Before being immersed in KOH, pure VAVTD polymer has three degradation steps. The first step occurs between 30 °C and 200 °C, with a 12 wt. % mass loss and is associated with the loss of internal water absorbed by the air's moisture. It is associated with internal water since it was not stored in an inert environment without moisture so that the membranes could absorb the environmental water. The second step occurs between 200 °C and 380 °C, with a maximum weight loss at 340 °C; at the end of this step the sample presents a 65 wt. % mass loss, this process could be related to the breakdown of the pendant groups[77]. The third step is taken from 350 °C onwards, reaching a maximum mass loss at 450 °C to finally reach a 5 wt. % of its initial weight at 540 °C which is maintained until the end of the test. This last step is related to the breaking of the copolymer backbone.

Restrepo et al.[75] identify three degradation steps for pure PVA. The first between 31 to 188 °C with a weight loss of 5%, the second between 190 and 388 °C with a weight loss between 65 and 77%, and the last step from 351 °C onwards with a weight loss of 95%.

VAVTD-PVA membranes without immersion present a behavior similar to pure VAVTD. However, the values of mass loss are lower. It can be attributed to the fact that pure PVA presents a higher thermal resistance than VAVTD. This affirmation can be corroborated in Santos et al[7]., where at a temperature of 350 °C, pure PVA presents a loss of 45% of its initial mass. In contrast, pure VAVTD at the same temperature presents a mass loss of 55%.

On the other hand, VAVTD-PVA GPEs immersed in KOH present very different curves than those that were not immersed, indicating a structural change. The first mass loss occurs from 30 °C to 135 °C and presents a higher mass loss than not immersed membranes, reaching a 20 wt.%. As shown in the thermogram's derivative located in the lower-left part of Figure 14, this first step reaches its maximum at a temperature of 100 °C. As in the rest of the membranes, it is associated with eliminating the free water.

The second mass loss occurs between 136 °C to 380 °C and is associated with the pendant groups' breakdown. It is essential to mention that in VAVTD-PVA membranes, before being submerged in KOH, the derivative shows that the point where a more significant weight loss occurs is at 340 °C. In contrast, when submerged, the point moves to lower temperatures reaching its maximum at 170 °C. This shift to lower temperatures is

associated with the high penetration of water and KOH molecules in the polymer matrix, generating many intermolecular interactions, as can be seen in Figure 11C).

Finally, the last mass loss occurs at 480 °C and is related to the backbone breakage of the copolymer. At the end, the GPEs preserve 40% of their original mass, which is associated with the formation of K_2O that according to Strydom et al. [78] is generated by the decomposition of KOH according to the equation 13:

$$2KOH(S) \rightarrow K_2O\ (s) + H_2O\ (g) \tag{13}$$
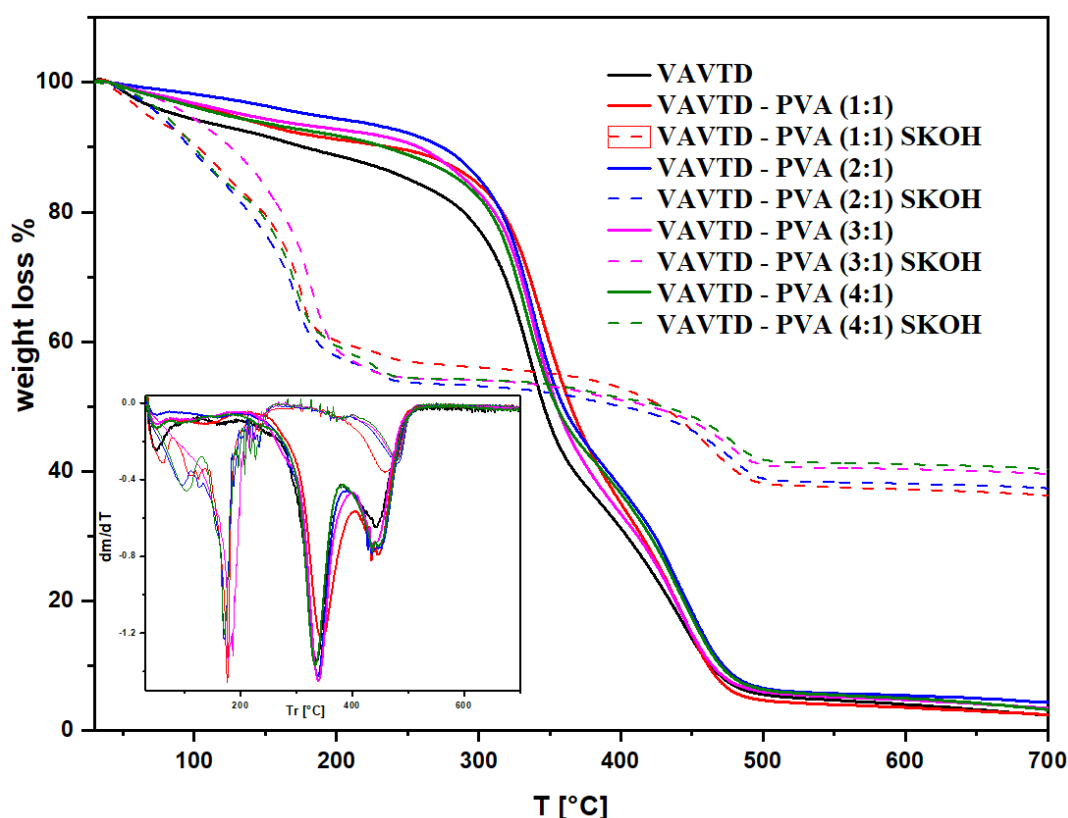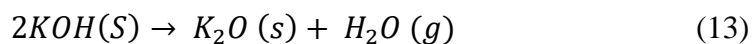
Figure 14 Thermogravimetric analysis and its derivative of VAVTD – PVA GPEs

As a result of the TGA analysis, we can conclude that VAVTD has a lower thermal resistance than PVA. In the same way, it was observed how incorporating KOH into the system contributes to the weakening of the thermal resistance due to its interaction with the pendant groups of the GPEs. This hypothesis finds support in the FITR and XRD analyzes, where the polymer chain in presence of a thermodynamically compatible solvent goes from a semi-crystalline state to a more thermodynamically favorable state

called "coil". Where the solvent penetrates the polymer matrix decrease its melting temperature, and increase its free volume.

5.3. Electrical and Electrochemical properties of the Gel Polymer Electrolytes

5.3.1. Temperature dependence of Ionic Conductivity

Table 6 Calculation of the ionic conductivity of GPE VAVTD -PVA (4: 1) submerged in KOH at different temperatures

Temperature °C	Temperature K	Area cm^2	Thickness cm	Resistance Ω	Ionic conductivity (σ) S $\cdot$ cm^{-1}	Ln (σ)
5	278.15	1	0.195	15.90	0.012	-4.401
10	283.15	1	0.195	12.80	0.015	-4.184
20	293.15	1	0.195	10.50	0.019	-3.986
30	303.15	1	0.195	10.10	0.019	-3.947
40	313.15	1	0.195	9.45	0.021	-3.881
50	323.15	1	0.195	8.47	0.023	-3.771
60	333.15	1	0.195	8.00	0.024	-3.714
70	343.15	1	0.195	7.77	0.025	-3.685

Table 6 presents the ionic conductivity of VAVTD-PVA (4: 1) GPE across a range of temperatures. As seen, the ionic conductivity (σ) obtained with equation 8 increases when the temperature of the sample rises, doubling its starting value (from 0.012 to 0.025 S cm^{-1}) at 70 °C. Similar works with hydrogels show ionic conductivity values of 0.0088 S cm^{-1} [79] and 0.015 S cm^{-1} [80] at room temperature.

Figure 15 A) presents a plot of $\ln(\sigma)$ vs $\frac{1000}{T}$ of VAVTD-PVA GPEs immersed in KOH. The curves observed presents an Arrhenius behavior (equation 9). From the slope generated in Figure 15 A) it is possible to obtain the activation energy of each membrane which is presented in the Figure 15 B). The activation energy (Ea) of the pure VAVTD GPEs is 0.071 eV and 0.073 eV for VAVTD - PVA (1: 1). The similarity of these values can lead us to suppose that the blending of VAVTD and PVA does not fulfill its purpose. However, from VAVTD - PVA (2: 1) GPE thereafter, the activation energy is reduced to less than half (0.034 eV) and remains constant despite increasing the VAVTD content.

From Figure 15 B) we can also deduce that increasing the VAVTD content in a GPEs also increases the ion conductivity. Starting from 0.004 Scm^{-1} in a 1:1 ratio to 0.019 S

cm^{-1} in a 4:1 ratio at room temperature (303.15 K). As mentioned in the qualities of a suitable electrolyte, high conductivity values are attractive for electrochemical applications and are related to a greater number of free ions moving through the polymer structure, which intervenes in the battery performance
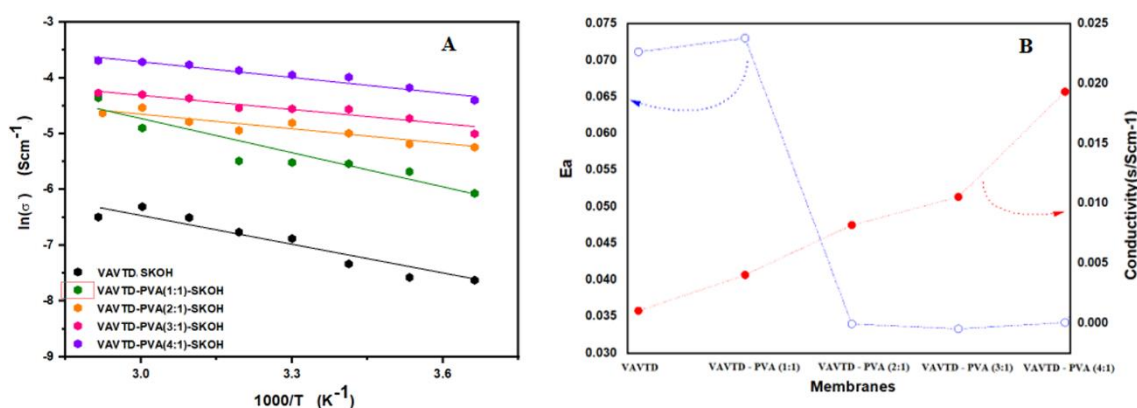
Figure 15 A) Variation of ionic conductivity with temperature for VAVTD-PVA B) Activation energy and conductivity of VAVTD – PVA

This phenomenon can be attributed to two factors:

1. As seen in Table 5, as the content of VAVTD increases, the swelling ratio also increases. This means that a greater number of KOH molecules penetrate the polymer and favors the ionic conductivity.
2. As observed in the X-ray diffraction analysis, the percentage of crystallinity of the GPE decreases with increasing VAVTD content. Increasing segmental movement and creating more free volume for ion transport, which is in agreement with the increasing of conductivity values.

It is also observed the membranes composed only of VAVTD have lower ionic conductivity and a higher Ea, although they present a higher KOH absorption (Table 5) than the rest of the membranes. This apparent contradictory result is explained by the weak mechanical and chemical resistance of pure VAVTD. Due to this, the importance of incorporating PVA into the sample can be seen.

5.3.2. Cyclic voltammetry (CV)
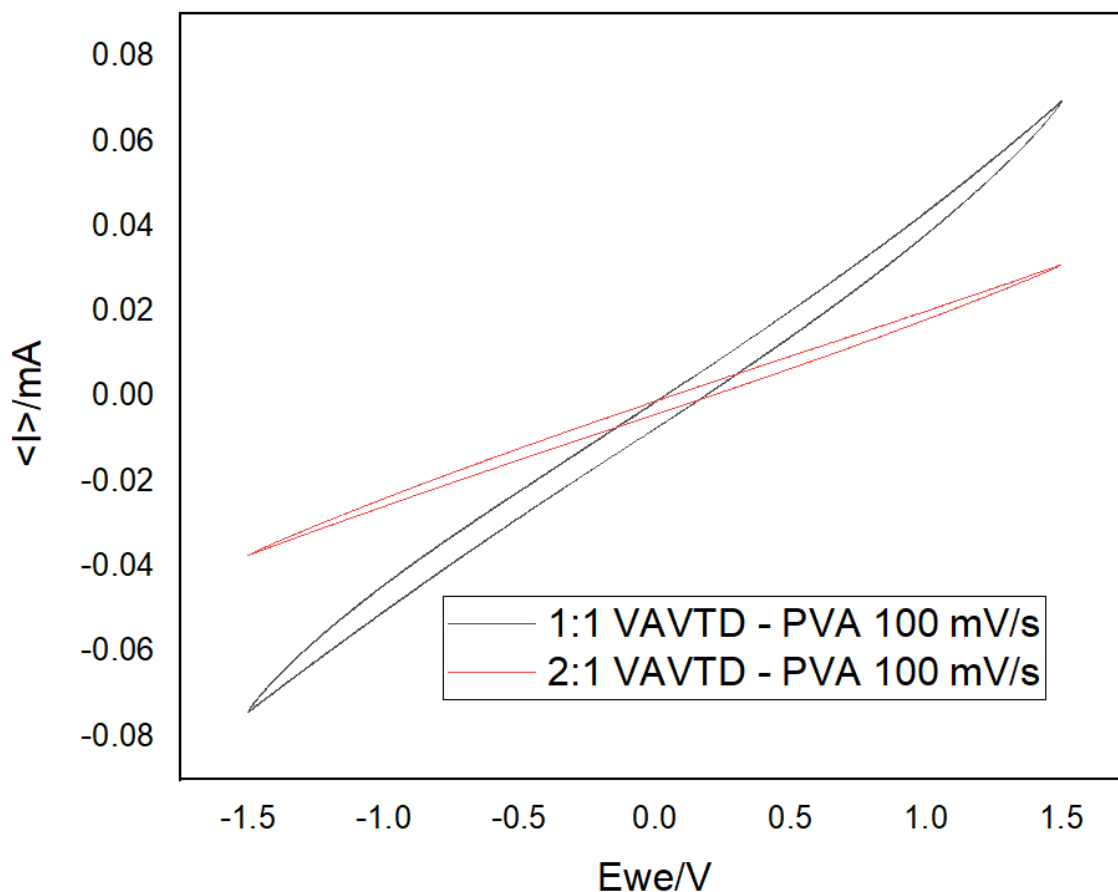

Figure 16 Cyclic voltammetry (CV) of VAVTD – PVA membranes in a Zn/ VAVTD – PVA/Zn cell.

Figure 16 shows the CV of VAVTD-PVA membranes without immersion in KOH. The capacitive voltammogram can be observed, which can be explained considering that no mobile ions are presented within the membrane, that does not allow the ionic transport to the electrode to compensate the redox reactions. Furthermore, these polymers behave like a bad electrolyte.

Figure 17 presents the electrochemical behavior of VAVTD-PVA membranes submerged in 12M KOH. It is observed that when the concentration of VAVTD increases the current density also increases. This phenomenon is associated with crystallinity reduction due to VAVTD and KOH presence and, consequently, the increase of ionic conductivity. A quasi-reversible behavior is observed for the oxidation/reduction processes; two anodic peaks (a, b) are presented, attributed to zinc oxidation to Zn^{2+} cations. On the other hand, the anodic peak (c) formed during the cathode sweep is due to greater oxidation of the Zn that takes place after the cathode scan dissolves the passive film formed in the Zn electrode[51].

The cathodic peak (a') is attributed to the reduction process of the Zn^{2+} species to Zn^0 [81]. Finally, it is suspected that the presence of the peak (c´) is related to the Zn / GPE / Zn configuration used to perform the test [7]. The bottom right of the image also presents 30 cycles of VAVTD - PVA (4: 1) GPE CV which shows the GPE stability.
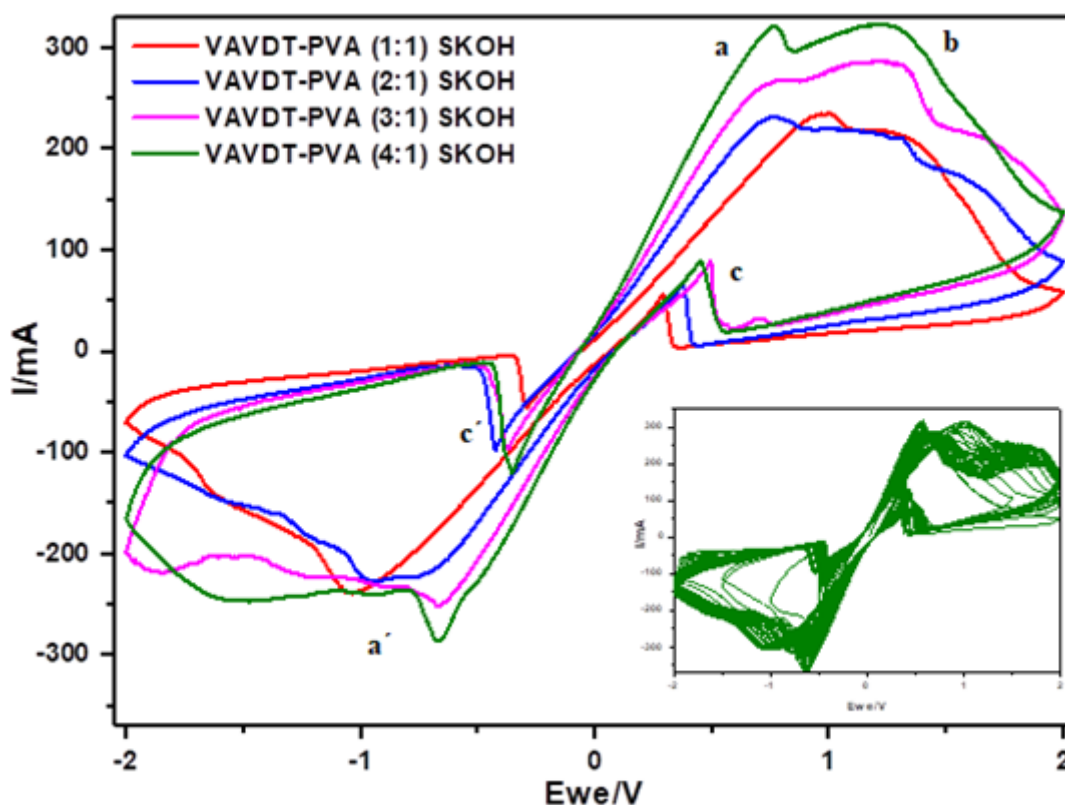
Figure 17 Cyclic voltammetry (CV) of VAVTD – PVA GPEs immersed in KOH 12M.

The present work's relevance can be observed in Figure 18 A) when comparing the CV intensity values obtained by Santos et al[7]. for GPEs based on pure PVA (PVA – KOH 30sw). The current intensity presents a maximum of 150 mA when immersed in KOH 12 M. However, this value represents the half of the one obtained in the present work for the GPEs VAVTD - PVA (4: 1) SKOH. As the current generated results from the transfer of electrons between the redox species and the electrode, which depends on the ions migration, increasing of current may be related to improvement of the ionic transfer through the GPE. Furthermore, VAVTD - PVA GPEs are presented as an alternative to consider in battery implementation. To determine if the GPEs retain the ions after undergoing a surface wash with distilled water, a CV analysis was carried out, the results of which are observed in Figure 18 B). The voltammogram shows that after being washed, the GPEs lose most of the free ions, making it a poor conductor.

Figure 18 A) Cyclic Voltammograms of VAVTD – PVA (4:1) SKOH and PVA-KOH 30 swollen membranes[7]. B) Cyclic Voltammograms of VAVTD – PVA GPEs before been washed
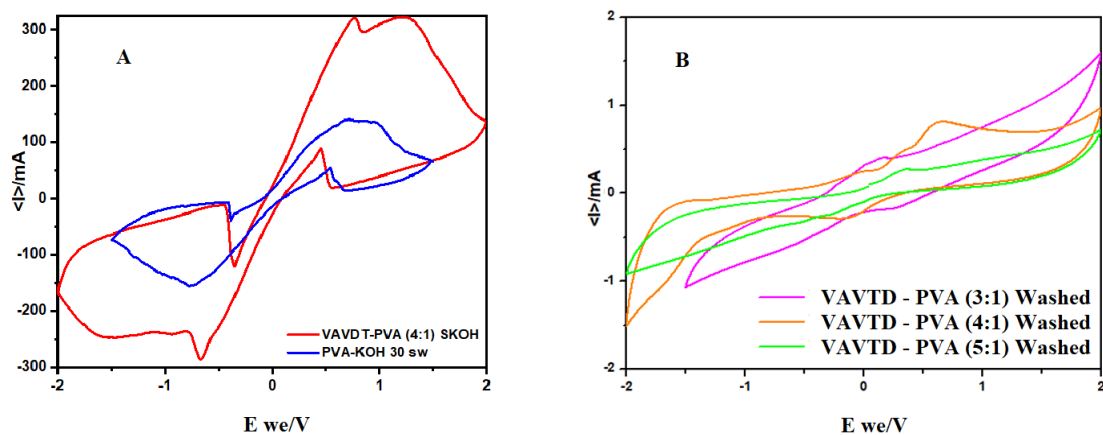
5.3.3. Zn /GPE/air Battery

Figure 19 shows a comparison between the discharge curves generated by the VAVTD-PVA GPEs (4: 1 and 5: 1) and the experimental data obtained by Santos et al.[7] for pure PVA-based GPE synthesized with 30 ml of KOH soaked in 12M KOH for 24h. Measurements were made with the Zn/GPE/air configuration using Zn powder as the anode and a discharge current of -5mA. It is important to emphasize that the result obtained by Santos et al.[7] was obtained using a Zn plate anode while those presented in this study used Zn powder.

PVA – KOH 30 presents a capacity of 110 mAh, and VAVTD -PVA GPEs present a capacity of 135 mAh and 150 mAh for (4:1) and (5:1) respectively at 0.9V. During the discharge process, we can observe that the GPE (4:1) maintains a stable potential between 1.1 and 1.2 V until reaching 95 mAh; then its potential is reduced to 0.9 V until reaching 135 mAh, where an abrupt fall begins. On the other hand, GPE (5:1) maintains a potential greater than (4: 1), reaching values between 1.2 and 1.3 V until reaching 150 mAh, where an abrupt fall begins. When performing a full discharge, the maximum capacity reaches 165 mAh and 195 mAh for (4: 1) and (5: 1) respectively.

The results obtained agree with the values obtained in the CV and conductivity tests where a high ion transport could be observed. Similarly, we can see that the best and more stable battery performance is found in the GPE (5: 1). This result is attributed to the high amorphous phase as well as the large number of ions absorbed in the GPE.
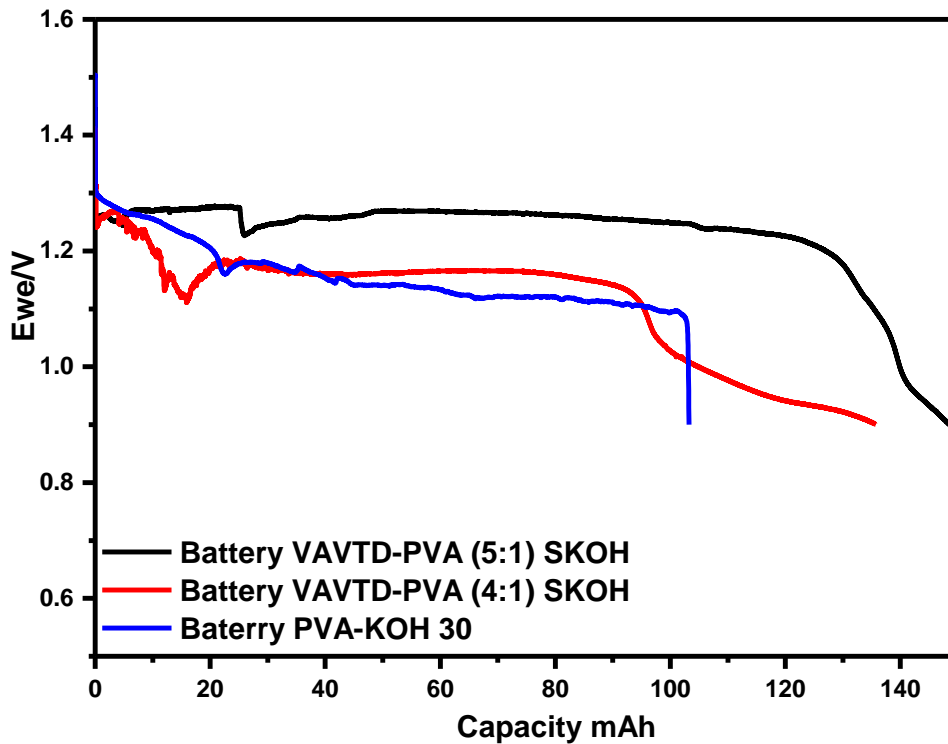
Figure 19 Zn/GPE/air batteries with VAVTD – PVA GPEs and pure PVA GPE

To improve the batteries performance, tests with mesoporous silica were carried out. The procedure used for the GPEs synthesis doped with silica was like the original one, adding the inert filler while the blend of VAVTD and PVA was stirring. The mixture was allowed to homogenize for 1 hour. Then was placed in a preti dish and cast at room temperature (30 °C) for one week. Mesoporous silica is known for being a material with poor conductivity. However, the main aim of using silica was to increase the void volume between polymeric chains inside the GPE, favoring the ionic movement. Besides, it can offer great benefits such as high adsorption capacity, increased surface area, and chemical, mechanical and thermal resistance when used in electrolytes and electrodes[82].

Figure 20 shows the discharge tests of silica-doped Zn/GPE/air batteries with a ratio of VAVTD-PVA-SILICA (4: 1: 0.5) and (5: 1: 0.5) immersed in KOH 12 M for 24 hours. It is observed that the maximum capacity rises to 250 mAh, which represents a substantial improvement compared to membranes without inert filler, presenting stable potential values up to 150 mAh. From this point on, the potentials stop being constant, and much interference starts to be generated in the battery's operation. These measurement problems can be generated by the non-optimization of the batteries' design. Therefore, it is recommended to increase the number of tests carried out.

This improvement in battery performance is attributed to the fact that the silica increases the void volume inside the polymer, probably helps to retain the KOH better and provides greater mechanical resistance than free-inert filler GPEs. Due to this, the study of GPEs with different inert fillers is promoted for a further work.
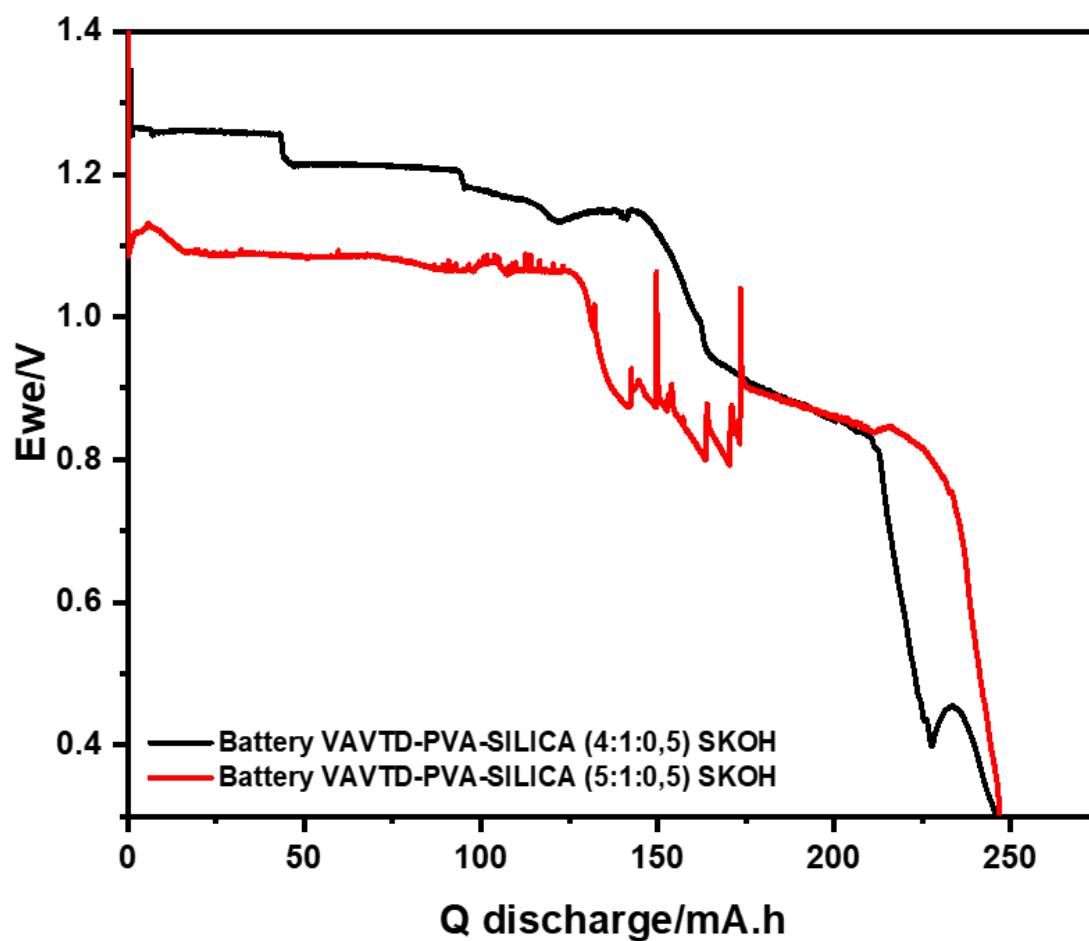

Figure 20 Zn/GPE/air batteries with VAVTD – PVA GPEs with silica inert filler.

6. CONCLUSION AND FUTURE WORK

The synthesis of GPEs was carried out using a blend of VAVTD and PVA, varying the concentration of VAVTD and keeping the concentration of PVA constant. The synthesized GPEs are a VAVTD - PVA ratio of (1: 1), (2: 1), (3: 1), (4: 1), and (5: 1). These GPEs were immersed for 24 hours in a 12M KOH solution.

The structural analysis of the GPEs result in swelling ratio (SR) values corresponding to a triple absorption of KOH and water when VAVTD was immersed in 12M KOH solution. However, it loses its mechanical strength and makes it difficult to use in batteries. That is why PVA has been added to reinforce the polymer matrix. Although the PVA adsorbs less KOH than VAVTD, it increases the overall strength of the GPE.

The X-ray diffraction and FTIR-ATR analysis demonstrate the interaction occurring between the polymer matrix of the GPEs and the water and KOH molecules. The semicrystalline structure of the membranes in contact with a thermodynamically compatible solvent (KOH) changes its structure to a more favorable one called "coil". In this structure, the solvent penetrates the polymer matrix, eliminating the internal crystals and increasing the amorphous zone. This zone increases the free volume of the GPE and facilitates segmental movements. It is observed that VAVTD has a less crystalline structure than PVA. Therefore, when its content in the synthesized GPEs increases, the total percentage of amorphousness increase also.

Thermogravimetric analysis reveals that conductivity of the GPEs increase with the amount of VAVTD incorporated to the membrane. Similarly, when the membranes are submerged in KOH, their thermal resistance is greatly affected due to the introduction of water and KOH molecules into the polymer matrix. This phenomenon is mainly evidenced in the shift of the pendant groups' breakdown temperature to a much lower value.

When analyzing the dependence of ionic conductivity with temperature, it was observed that the GPEs present an Arrhenius-type behavior. Besides, the increasing of VAVTD content produces higher conductivity values as well as lower Activation Energy (Ea) values. This behavior was related to the reduction of crystallinity of the sample and the greater number of ionic species inside the polymeric matrix.

Cyclic voltammetry tests verified the advantages of GPEs based on VAVTD and PVA compared to those formed only by PVA, doubling the values reported by previous research teams. The high-intensity values presented suggested a high electron transfer between the redox species and the electrode. Similarly, a quasi-reversible behavior was observed in the oxidation and reduction processes, which suggests the possible application in rechargeable batteries.

The Zn/GPE/air batteries presented maximum capacity values 40% greater than those presented by previous research groups based on PVA. That is due to the increase of the amorphous phase, the polymeric matrix free volume, and the higher absorption of KOH by the GPE. Similarly, the silica implementation as an inert filler improved the batteries' performance, which may be attributed to the increasing of void volume between polymeric chains, higher capacity to retain KOH and the increased surface area generated.

It is recommended to continue with research in battery development since, throughout the year 2020, humanity's technological dependence has been evidenced. VAVTD has proven to be a material with great aspirations to be implemented in batteries. Therefore, it is recommended to continue with this research. Besides, due to the results presented here, it is proposed to study the behavior of VAVTD when it is blended with other polymers such as PEO, PMMA, PVC and PVdf-HDF.

The exploration of different composites such as inert ceramic fillers, fast-ion conductive ceramics, ionic liquids, and cellulose can provide a broad field of research for VAVTD. That is why its investigation is recommended for future works.

7. BIBLIOGRAPHY

1.	Zhong H, Li K, Zhang Q, et al. In situ anchoring of Co9S8 nanoparticles on N and S co-doped porous carbon tube as bifunctional oxygen electrocatalysts. *NPG Asia Mater*. 2016;8(9):e308-e308. doi:10.1038/am.2016.132

2.	Young K, Wang C, Wang LY, Strunz K. Electric Vehicle Battery Technologies. In: *Electric Vehicle Integration into Modern Power Networks*. Springer New York; 2013:15-56. doi:10.1007/978-1-4614-0134-6_2

3.	EuropeanCommission. EU Battery Alliance: regions join forces to build a strong industrial value chain in advanced materials for batteries. Published 2018. Accessed July 1, 2020. https://ec.europa.eu/regional_policy/en/newsroom/news/2018/10/10-08-2018-eu-battery-alliance-regions-join-forces-to-build-a-strong-industrial-value-chain-in-advanced-materials-for-batteries

4.	Schofield H. Coronavirus: France announces €8bn rescue plan for car industry. *BBC*. 2020:2.

5.	Pal R, Bhadada SK. Cash, currency and COVID-19. *Postgrad Med J*. Published online 2020:19-20. doi:10.1136/postgradmedj-2020-138006

6.	Lorca S. Síntesis y Caracterización de Electrodos de Óxidos Metálicos para su uso en baterías de Zinc. Published online 2019.

7.	Santos F, Tafur JP, Abad J, Fernández Romero AJ. Structural modifications and ionic transport of PVA-KOH hydrogels applied in Zn/Air batteries. *J Electroanal Chem*. 2019;850:113380. doi:10.1016/j.jelechem.2019.113380

8.	Inzelt G. Crossing the bridge between thermodynamics and electrochemistry. From the potential of the cell reaction to the electrode potential. *ChemTexts*. 2015;1(1):1-11. doi:10.1007/s40828-014-0002-9

9.	Lin D, Liu Y, Cui Y. Reviving the lithium metal anode for high-energy batteries. *Nat Nanotechnol*. 2017;12(3):194-206. doi:10.1038/nnano.2017.16

10.	Li Y, Lu J. Metal-Air Batteries: Will They Be the Future Electrochemical Energy Storage Device of Choice? *ACS Energy Lett*. 2017;2(6):1370-1377. doi:10.1021/acsenergylett.7b00119

11.	Li L, Chang Z, Zhang X-B. Recent Progress on the Development of Metal-Air Batteries. *Adv Sustain Syst*. 2017;1(10):1700036. doi:10.1002/adsu.201700036

12.	Yu T, Fu J, Cai R, Yu A, Chen Z. Nonprecious Electrocatalysts for Li?Air and Zn?Air Batteries: Fundamentals and recent advances. *IEEE Nanotechnol Mag*. 2017;11(3):29-55. doi:10.1109/MNANO.2017.2710380

13.	Sun X, Hao H, Zhao F, Liu Z. Global Lithium Flow 1994-2015: Implications for Improving Resource Efficiency and Security. *Environ Sci Technol*. 2018;52(5):2827-2834. doi:10.1021/acs.est.7b06092

14.	Pan J, Xu YY, Yang H, Dong Z, Liu H, Xia BY. Advanced Architectures and Relatives of Air Electrodes in Zn–Air Batteries. *Adv Sci*. 2018;5(4). doi:10.1002/advs.201700691

15.   Fu J, Cano ZP, Park MG, Yu A, Fowler M, Chen Z. Electrically Rechargeable Zinc–Air Batteries: Progress, Challenges, and Perspectives. *Adv Mater*. 2017;29(7). doi:10.1002/adma.201604685

16.   Cheng H, Chen JM, Li QJ, et al. A modified molecular framework derived highly efficient Mn-Co-carbon cathode for a flexible Zn-air battery. *Chem Commun*. 2017;53(84):11596-11599. doi:10.1039/c7cc04099g

17.   Khor A, Leung P, Mohamed MR, et al. Review of zinc-based hybrid flow batteries: From fundamentals to applications. *Mater Today Energy*. 2018;8:80-108. doi:10.1016/j.mtener.2017.12.012

18.   Tomboc GM, Yu P, Kwon T, Lee K, Li J. Ideal design of air electrode—A step closer toward robust rechargeable Zn–air battery. *APL Mater*. 2020;8(5):050905. doi:10.1063/5.0005137

19.   Sun H, Liu S, Wang M, Qian T, Xiong J, Yan C. Updating the Intrinsic Activity of a Single-Atom Site with a P-O Bond for a Rechargeable Zn-Air Battery. *ACS Appl Mater Interfaces*. 2019;11(36):33054-33061. doi:10.1021/acsami.9b11337

20.   Santos F, Urbina A, Abad J, López R, Toledo C, Fernández Romero AJ. Environmental and economical assessment for a sustainable Zn/air battery. *Chemosphere*. 2020;250. doi:10.1016/j.chemosphere.2020.126273

21.   Wang HF, Tang C, Zhang Q. A Review of Precious-Metal-Free Bifunctional Oxygen Electrocatalysts: Rational Design and Applications in Zn−Air Batteries. *Adv Funct Mater*. 2018;28(46):1-22. doi:10.1002/adfm.201803329

22.   Cheng X, Pan J, Zhao Y, Liao M, Peng H. Gel Polymer Electrolytes for Electrochemical Energy Storage. *Adv Energy Mater*. 2018;8(7):1-16. doi:10.1002/aenm.201702184

23.   Kumar SA, Kuppusami P. *Enhancing the Ionic Conductivity in the Ceria-Based Electrolytes for Intermediate Temperature Solid Oxide Fuel Cells*. INC; 2019. doi:10.1016/B978-0-12-817445-6.00005-3

24.   Aziz SB, Woo TJ, Kadir MFZ, Ahmed HM. A conceptual review on polymer electrolytes and ion transport models. *J Sci Adv Mater Devices*. 2018;3(1):1-17. doi:10.1016/j.jsamd.2018.01.002

25.   Yao P, Yu H, Ding Z, et al. Review on Polymer-Based Composite Electrolytes for Lithium Batteries. *Front Chem*. 2019;7(August):1-17. doi:10.3389/fchem.2019.00522

26.   Fenton DE, Parker JM, Wright P V. Complexes of alkali metal ions with poly(ethylene oxide). *Polymer (Guildf)*. 1973;14(11):589. doi:10.1016/0032-3861(73)90146-8

27.   Ngai KS, Ramesh S, Ramesh K, Juan JC. A review of polymer electrolytes: fundamental, approaches and applications. *Ionics (Kiel)*. 2016;22(8):1259-1279. doi:10.1007/s11581-016-1756-4

28.   Manthiram A, Yu X, Wang S. Lithium battery chemistries enabled by solid-state electrolytes. *Nat Rev Mater*. 2017;2(4):1-16. doi:10.1038/natrevmats.2016.103

29.   Long L, Wang S, Xiao M, Meng Y. Polymer electrolytes for lithium polymer

batteries. *J Mater Chem A*. 2016;4(26):10038-10039. doi:10.1039/c6ta02621d

30. Mauger A, Julien CM, Goodenough JB, Zaghib K. Tribute to Michel Armand: from Rocking Chair – Li-ion to Solid-State Lithium Batteries. *J Electrochem Soc*. 2020;167(7):070507. doi:10.1149/2.0072007jes

31. Arya A, Sharma AL. *Polymer Electrolytes for Lithium Ion Batteries: A Critical Study*. Vol 23. Ionics; 2017. doi:10.1007/s11581-016-1908-6

32. Polu AR, Kumar R. Preparation and characterization of pva based solid polymer electrolytes for electrochemical cell applications. *Chinese J Polym Sci (English Ed*. 2013;31(4):641-648. doi:10.1007/s10118-013-1246-3

33. Liang B, Jiang Q, Tang S, Li S, Chen X. Porous polymer electrolytes with high ionic conductivity and good mechanical property for rechargeable batteries. *J Power Sources*. 2016;307:320-328. doi:10.1016/j.jpowsour.2015.12.127

34. Han HS, Kang HR, Kim SW, Kim HT. Phase-separated polymer electrolyte based on poly(vinyl chloride)/poly(ethyl methacrylate) blend. *J Power Sources*. 2002;112(2):461-468. doi:10.1016/S0378-7753(02)00436-6

35. Lin D, Liu W, Liu Y, et al. High Ionic Conductivity of Composite Solid Polymer Electrolyte via in Situ Synthesis of Monodispersed SiO2 Nanospheres in Poly(ethylene oxide). *Nano Lett*. 2016;16(1):459-465. doi:10.1021/acs.nanolett.5b04117

36. Kuo CW, Li W Bin, Chen PR, Liao JW, Tseng CG, Wu TY. Effect of plasticizer and lithium salt concentration in PMMA-based composite polymer electrolytes. *Int J Electrochem Sci*. 2013;8(4):5007-5021.

37. Li Y, Wang J, Tang J, Liu Y, He Y. Conductive performances of solid polymer electrolyte films based on PVB/LiClO4 plasticized by PEG200, PEG400 and PEG600. *J Power Sources*. 2009;187(2):305-311. doi:10.1016/j.jpowsour.2008.11.126

38. Amaral FA, Sousa RM, Morais LCT, et al. Preparation and characterization of the porous solid polymer electrolyte of PAN/PVA by phase inversion. *J Appl Electrochem*. 2015;45(8):809-820. doi:10.1007/s10800-015-0816-1

39. Zhang Q, Liu K, Ding F, Liu X. Recent advances in solid polymer electrolytes for lithium batteries. *Nano Res*. 2017;10(12):4139-4174. doi:10.1007/s12274-017-1763-4

40. Shi J, Yang Y, Shao H. Co-polymerization and blending based PEO/PMMA/P(VDF-HFP) gel polymer electrolyte for rechargeable lithium metal batteries. *J Memb Sci*. 2018;547(September 2017):1-10. doi:10.1016/j.memsci.2017.10.033

41. Jadoun S, Riaz U. A review on the chemical and electrochemical copolymerization of conducting monomers: recent advancements and future prospects. *Polym Technol Mater*. 2020;59(5):484-504. doi:10.1080/25740881.2019.1669647

42. Zhou D, Shanmukaraj D, Tkacheva A, Armand M, Wang G. Polymer Electrolytes for Lithium-Based Batteries: Advances and Prospects. *Chem*. 2019;5(9):2326-2352. doi:10.1016/j.chempr.2019.05.009

43. Feuillade G, Perche P. Ion-conductive macromolecular gels and membranes. *J Appl Electrochem*. 1975;5:63-69.

44. Na R, Liu Y, Lu N, Zhang S, Liu F, Wang G. Mechanically robust hydrophobic association hydrogel electrolyte with efficient ionic transport for flexible supercapacitors. *Chem Eng J*. 2019;374(May):738-747. doi:10.1016/j.cej.2019.06.004

45. Ramesh S, Liew CW, Ramesh K. Evaluation and investigation on the effect of ionic liquid onto PMMA-PVC gel polymer blend electrolytes. *J Non Cryst Solids*. 2011;357(10):2132-2138. doi:10.1016/j.jnoncrysol.2011.03.004

46. Agrawal SL, Awadhia A. DSC and conductivity studies on PVA based proton conducting gel electrolytes. *Bull Mater Sci*. 2004;27(6):523-527. doi:10.1007/BF02707280

47. Lian F, Wen Y, Ren Y, Guan HY. A novel PVB based polymer membrane and its application in gel polymer electrolytes for lithium-ion batteries. *J Memb Sci*. 2014;456:42-48. doi:10.1016/j.memsci.2014.01.010

48. Wang SH, Hou SS, Kuo PL, Teng H. Poly(ethylene oxide)-co-poly(propylene oxide)-based gel electrolyte with high ionic conductivity and mechanical integrity for lithium-ion batteries. *ACS Appl Mater Interfaces*. 2013;5(17):8477-8485. doi:10.1021/am4019115

49. Kim DW. Electrochemical characterization of poly(ethylene-co-methyl acrylate)-based gel polymer electrolytes for lithium-ion polymer batteries. *J Power Sources*. 2000;87(1):78-83. doi:10.1016/S0378-7753(99)00363-8

50. Xiao W, Li X, Wang Z, Guo H, Li Y, Yang B. Performance of PVDF-HFP-based gel polymer electrolytes with different pore forming agents. *Iran Polym J (English Ed*. 2012;21(11):755-761. doi:10.1007/s13726-012-0081-7

51. Tafur JP, Santos F, Fernández Romero AJ. Influence of the ionic liquid type on the gel polymer electrolytes properties. *Membranes (Basel)*. 2015;5(4):752-771. doi:10.3390/membranes5040752

52. Armand Michel. Polymers with Ionic Conductivity (Pol. *Adv Mater*. 1990;2(617):278-286.

53. Meyer WH. Polymer Electrolytes for Lithium-Ion Batteries. *Adv Mater*. 1998;10(6):439-448. doi:10.1002/(SICI)1521-4095(199804)10:6<439::AID-ADMA439>3.0.CO;2-I

54. Kumar A, Han SS. PVA-based hydrogels for tissue engineering: A review. *Int J Polym Mater Polym Biomater*. 2017;66(4):159-182. doi:10.1080/00914037.2016.1190930

55. Inoue H. Hydrogel Electrolyte. In: Kreysa G, Ota K, Savinell RF, eds. *Encyclopedia of Applied Electrochemistry*. Springer New York; 2014:1035-1039. doi:10.1007/978-1-4419-6996-5_515

56. Popov BN. Organic Coatings. In: *Corrosion Engineering*. Elsevier; 2015:557-579. doi:10.1016/B978-0-444-62722-3.00013-6

57. Ovando-Medina VM, Díaz-Flores PE, Peralta RD, Mendizábal E, Cortez-

Mazatan GY. Semicontinuous heterophase copolymerization of vinyl acetate and butyl acrylate. *J Appl Polym Sci*. 2013;127(4):2458-2464. doi:10.1002/app.37943

58.   Agirre A, Weitzel HP, Hergeth WD, Asua JM. Process intensification of VAc-VeoVa10 latex production. *Chem Eng J*. 2015;266:34-47. doi:10.1016/j.cej.2014.12.053

59.   Díaz-Barrios A, González G, Reinoso C, et al. In situ synthesis and long-term stabilization of nanosilver in poly(vinyl acetate-co-butyl acrylate-co-neodecanoate) matrix for antibacterial applications. *Mater Chem Phys*. 2020;255:123476. doi:10.1016/j.matchemphys.2020.123476

60.   Santiana J. DESARROLLO DE UNA EMULSIÓN POLIMÉRICA VINIL-ACRÍLICA CON CARACTERÍSTICAS HIDROFÓBICAS. Published online 2017.

61.   Dunlap RA. X-ray diffraction techniques. *Nov Microstruct Solids*. Published online 2018:215-237. doi:10.1088/2053-2571/aae653ch2

62.   Ismail AS, Darwish MSA, Ismail EA. Synthesis and characterization of hydrophilic chitosan-polyvinyl acetate blends and their sorption performance in binary methanol–water mixture. *Egypt J Pet*. 2017;26(1):17-22. doi:10.1016/j.ejpe.2016.02.006

63.   Aziz SB, Abdulwahid RT, Rasheed MA, Abdullah OGH, Ahmed HM. Polymer blending as a novel approach for tuning the SPR peaks of silver nanoparticles. *Polymers (Basel)*. 2017;9(10):486. doi:10.3390/polym9100486

64.   Gupta S, Pramanik AK, Kailath A, et al. Composition dependent structural modulations in transparent poly(vinyl alcohol) hydrogels. *Colloids Surfaces B Biointerfaces*. 2009;74(1):186-190. doi:10.1016/j.colsurfb.2009.07.015

65.   Zelkó R, Szakonyi G. The effect of water on the solid state characteristics of pharmaceutical excipients: Molecular mechanisms, measurement techniques, and quality aspects of final dosage form. *Int J Pharm Investig*. 2012;2(1):18. doi:10.4103/2230-973x.96922

66.   Nonappa, Kolehmainen E. Solid state NMR studies of gels derived from low molecular mass gelators. *Soft Matter*. 2016;12(28):6015-6026. doi:10.1039/c6sm00969g

67.   Tranter GE. *FTIR Spectroscopy of Aqueous Solutions*. 3rd ed. Elsevier Ltd.; 2016. doi:10.1016/B978-0-12-409547-2.12157-2

68.   Costa VC, Costa HS, Vasconcelos WL, Pereira M de M, Oréfice RL, Mansur HS. Preparation of hybrid biomaterials for bone tissue engineering. *Mater Res*. 2007;10(1):21-26. doi:10.1590/S1516-14392007000100006

69.   Liu H, Bian J, Wang Z, Hou CJ. Synthesis and characterization ofwaterborne fluoropolymers prepared by the one-step semi-continuous emulsion polymerization of chlorotrifluoroethylene, vinyl acetate, butyl acrylate, veova 10 and acrylic acid. *Molecules*. 2017;22(1). doi:10.3390/molecules22010184

70.   Almafie MR, Nawawi Z, Jauhari J, Sriyanti I. Electrospun of Poly (vinyl alcohol)/Potassium hydroxide (PVA/KOH) nanofiber composites using the electrospinning method. *IOP Conf Ser Mater Sci Eng*. 2020;850(1).

doi:10.1088/1757-899X/850/1/012051

71. Szymanska-Chargot M, Zdunek A. Use of FT-IR Spectra and PCA to the Bulk Characterization of Cell Wall Residues of Fruits and Vegetables Along a Fraction Process. *Food Biophys*. 2013;8(1):29-42. doi:10.1007/s11483-012-9279-7

72. Qiao J, Fu J, Lin R, Ma J, Liu J. Alkaline solid polymer electrolyte membranes based on structurally modi fi ed PVA / PVP with improved alkali stability. *Polymer (Guildf)*. 2010;51(21):4850-4859. doi:https://doi.org/10.1016/j.polymer.2010.08.018 47

73. Fu J, Qiao J, Lv H, Ma J. *Alkali Doped Poly(Vinyl Alcohol) (PVA) for Anion-Exchange Membrane Fuel Cells - Ionic Conductivity, Chemical Stability and FT-IR Characterizations.* Vol 25.; 2010. doi:https://doi.org/10.1149/1.3315169.

74. Reichenbacher M, Popp J. *Challenges in Molecular Structure Determination*. Springer New York doi:10.1007/978-3-642-24390-5

75. Restrepo I, Medina C, Meruane V, Akbari-Fakhrabadi A, Flores P, Rodríguez-Llamazares S. The effect of molecular weight and hydrolysis degree of poly(vinyl alcohol)(PVA) on the thermal and mechanical properties of poly(lactic acid)/PVA blends. *Polimeros*. 2018;28(2):169-177. doi:10.1590/0104-1428.03117

76. Das O, Kim NK, Hedenqvist MS, Bhattacharyya D. *The Flammability of Biocomposites*.; 2018. doi:10.1016/B978-0-08-102290-0.00015-5

77. Duquesne S, Lefebvre J, Delobel R, Camino G, LeBras M, Seeley G. Vinyl acetate/butyl acrylate copolymers - Part 1: Mechanism of degradation. *Polym Degrad Stab*. 2004;83(1):19-28. doi:10.1016/S0141-3910(03)00176-9

78. Strydom CA, Collins AC, Bunt JR. The influence of various potassium compound additions on the plasticity of a high-swelling South African coal under pyrolyzing conditions. *J Anal Appl Pyrolysis*. 2015;112:221-229. doi:10.1016/j.jaap.2015.01.023

79. Liu X, Yin C, Yang J, et al. Controllable preparation of an eggshell membrane supported hydrogel electrolyte with thickness-dependent electrochemical performance. *J Mater Chem A*. 2016;4(46):17933-17938. doi:10.1039/c6ta07341g

80. Liao H, Zhou F, Zhang Z, Yang J. A self-healable and mechanical toughness flexible supercapacitor based on polyacrylic acid hydrogel electrolyte. *Chem Eng J*. 2019;357:428-434. doi:10.1016/j.cej.2018.09.153

81. Dergacheva MB, Urazov KA, Khussurova GM, Leontyeva KA. New method of pulsed electrodeposition of nanostructure of ZnS films. *Coatings*. 2016;6(2). doi:10.3390/coatings6020014

82. Sacara AM, Nairi V, Salis A, Turdean L. Silica-Modified Electrodes for Electrochemical Detection of Malachite Green. Published online 2017:1-9. doi:10.1002/elan.201700400